

UNIVERSITA' DEGLI STUDI DI NAPOLI FEDERICO II

Dipartimento di Medicina Clinica e Chirurgia



**DOTTORATO DI RICERCA IN
TERAPIE AVANZATE BIOMEDICHE E
CHIRURGICHE**

31° CICLO

**“Investigating the role of Hedgehog signaling in triple negative
breast cancer microenvironment ”**

Relators

Ch.mo Prof. Sabino De Placido

Ch.mo Prof. Roberto Bianco

Candidate

Dott.ssa Concetta Di Mauro

ANNO ACCADEMICO 2017-2018

INDEX

1. Introduction

1.1 Therapeutic Options for TNBC

1.2 The Hedgehog (Hh) signaling pathway

1.3 HH pathway and cancer microenvironment

2. Study purpose

3. Materials and Methods

4. Results

4.1 Task 1:

- **GLI1 is frequently overexpressed in TNBC primary and immortalized cell lines.**
- **GLI1 expression in TNBC patients**

4.2 Task2:

- **GLI1 expression correlates with VEGFR2 in TNBC patients**
- **Hh pathway regulates the production of pro- and anti-angiogenic secreted factors.**
- **GLI1 regulates VEGFR2 expression.**
- **NVP-LDE225 increases the efficacy of paclitaxel in nude mice xenografted with TNBC tumors.**

4.3 Task 3:

- **GLI1 expression correlates with PDL1 in TNBC patients**
- **GLI1 regulates PDL1 expression in TNBC cell lines.**

5. Discussion

6. References

1. Introduction

Breast cancer is a genetically and clinically heterogeneous disease. Based on this heterogeneity, breast cancer can be classified according to the presence and expression of three molecular markers: estrogen receptor (ER), progesterone receptor (PgR) and human epidermal growth factor receptor 2 (HER2). These classification schemes have evolved over many decades into a useful tool for treatment choices and patients prognosis.

Triple-negative breast cancer (TNBC) is an aggressive histological subtype characterized by a lack of ER, PR, and HER2 receptors. TNBC accounts for 10-17% of all breast carcinomas (Haffty et al, 2006; Penault-Llorca and Viale, 2012), it is often correlated with shorter disease-free and overall survival compared with those of women affected by non-TNBC (Dent et al., 2007; Liedtke et al., 2008).

Extensive genomic studies of breast tumors have identified distinct groups with differences in survival and response to therapy, establishing five major breast cancer intrinsic subtypes:

- luminal A, characterized by the presence of ER and PgR but with low or absent HER2 expression,
- luminal B, triple positive for ER, PgR and HER2;
- HER2-enriched, characterized by the absence of ER and PgR but HER2 positive;
- basal-like, triple negative for ER-/PgR-/HER2 and showing Basal Markers.
- claudin-low, characterized by low to absent expression of luminal differentiation markers, high enrichment for epithelial-to-mesenchymal transition markers, immune response genes and cancer stem cell like features.

After the advent of genomic analysis and the subtyping of breast cancers according to gene expression profiles many have used the terms TNBC and “basal-like” as synonymous. However, the spectrum of TNBC is heterogeneous: While 75% to 80% of TNBC cases correlate with the “basal” or “claudin-low” subtypes, about 9% are HER2-positive, and 11% have some hormone receptor gene expression (5% luminal A; 6% luminal B) (Figure 1). However, clinically decisions are based upon the

immunohistochemical profile of a tumor is obtained, which, in the case of TNBC, is marked by the absence of the three commonly tested receptors.

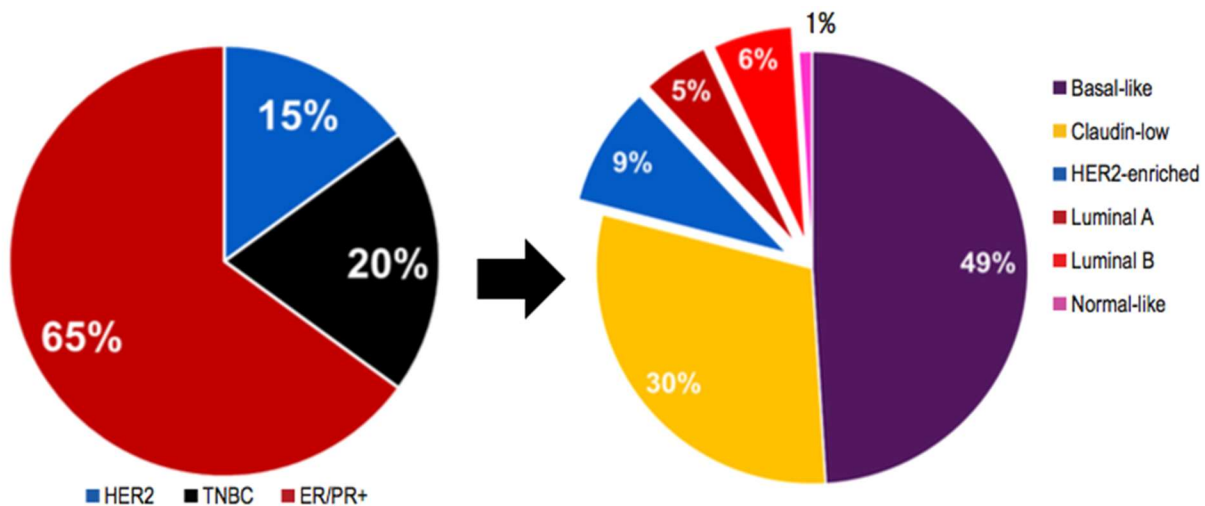


Figure 1. Breast cancer subtypes. Triple-negative breast cancer (TNBC) accounts for 10% to 20%, HER2 positive for about 15% and ER/PgR positive for 65% of all breast cancers. While 75% to 80% of TNBC cases correlate with the “basal” or “claudin-low” subtypes, about 9% are HER2-positive, and 11% have some hormone receptor gene expression.

1.1 Therapeutic options for TNBC

Given the lack of ERs, PgRs, and HER2 receptors, options for systemic therapy in TNBC are limited. Chemotherapy remains the main therapeutic option for TNBC patients, since neither endocrine therapies nor HER2 targeted agents are effective. Due to poor prognosis and restricted therapeutic chances (Chacón and Costanzo, 2010; Palma et al., 2015), new targeted therapies for TNBC are required to improve the outcome of this subset of breast cancer. A number of agents have been and are being evaluated for use in TNBC.

PARP (poly ADP ribose polymerase) is involved in repairing single-stranded DNA breaks, and it has therefore been hypothesized that PARP inhibition may cause cell death by preventing repair of

mutated DNA within cancer cells. Several studies found no objective response with PARP inhibitors in unselected TNBC patients (Liu JF et al., 2013)

Several studies have evaluated antiangiogenic agents, such as the VEGF inhibitor bevacizumab. Published data have shown that TNBC tumors express high levels of intratumoral Vascular Endothelial Growth Factor (VEGF) (Linderholm et al., 2009), possess high microvessel density (Mohammed et al., 2011) and display VEGF gene amplification compared to non-TNBC tumors (André et al., 2009), suggesting a marked angiogenic dependency in TNBC tumorigenesis and a potential sensitivity to anti-angiogenic agents. In fact, results of studies of bevacizumab in the neoadjuvant setting have demonstrated an improvement in pathologic complete response (pCR) rates (von Minckwitz et al., 2012) The treatment with the anti-VEGF monoclonal antibody (mAb) bevacizumab has shown some benefit when combined with standard chemotherapy (Bear et al. 2012) albeit the therapeutic use of bevacizumab and its clinical relevance in TNBC treatment is in the center of a controversy. As matter of fact, several studies demonstrated an approximate doubling of progression-free survival (PFS) compared with placebo despite no benefit in overall survival (OS) associated with the use of bevacizumab was obtained (Gray R, 2009; Miles DW 2010; Robert NJ, 2011).

One of the most exciting therapeutic developments, however, has been in the area of immunotherapy. Cancer immunotherapy represents a novel tool for cancer treatment based on the idea that stimulation of immune system may help to fight tumor. In comparison to conventional therapies for cancer, immunotherapy targets the immune system or tumor microenvironment rather than tumor cells themselves and can produce a synergistic effect in combination therapies (Whiteside et al., 2016).

Immune checkpoints are crucial pathways for self-tolerance, which prevents the immune system from attacking cells indiscriminately. The blockade of checkpoints such as cytotoxic T lymphocyte-associated antigen 4 (CTLA-4), programmed death 1 (PD-1) receptor and programmed death 1 receptor ligand (PD-L1) can inhibit tumor immunoescape.

Studies of meta-analysis indicate that PD-L1 expression was associated with positive lymph node metastasis, higher histological grades, estrogen receptor (ER)-negativity, and triple-negative breast cancer (TNBC). Moreover TNBCs have high level of tumor-infiltrating lymphocytes (TIL), suggesting that these tumors may be particularly amenable to targeting with immune checkpoint inhibitors (Stanton et al., 2016). Currently, several ongoing studies are investigating the use of immune checkpoints, including CTLA-4 and PD-1 pathways, as potential targets of therapy for breast cancer in the neoadjuvant setting. Furthermore targeting PD-L1, especially within the TNBC subset, has been of particular interest (Yu L Y et al. 2017).

1.2 The Hedgehog (Hh) signaling pathway

The Hedgehog (Hh) signalling, initially discovered in *Drosophila melanogaster*, is an evolutionarily conserved pathway (Ingham et al., 2001); it is broadly active in early embryonic development, playing a crucial role in cell proliferation and differentiation, regulating angiogenesis and vascular formation and orchestrating tissue patterning in vertebrates and invertebrates (Van den Brink et al., 2007; Pak and Segal, 2016; Nagase et al., 2008)

Later in life, Hh signaling is however inactive and, in adulthood, it presumably maintains stem cell populations and/or early progenitor cells.

The key components of the mammalian Hh pathway consist of three secreted ligands (Sonic Hedgehog (SHH), Indian Hedgehog (IHH) and Desert Hedgehog (DHH)), a 12-pass transmembrane receptor (Patched (PTCH)), a negative regulator Suppressor of fused homolog (SUFU), a positive regulatory protein Smoothed (SMO) and the glioma-associated oncogene (GLI) transcription factors (GLI1, GLI2 and GLI3) (Varjosalo, and Taipale, 2008) .

Without the Hh signal, GLI1 and GLI2 transcription factors are sequestered by SUFU in the cytoplasm; the repressor factor GLI3 full length (gli3FL) is complexed with SUFU leading to the efficient processing of GLI3FL into GLI3 Repressor and the cell is maintained in a neutral state. When Hh

signaling is initiated, ligands bind to PTCH, the inhibition of SMO by PTCH is relieved and activated SMO in turn initiates a downstream signalling cascade leading to the release of GLI1 transcription factor from SUFU-mediated cytoplasmic sequestration and activation of GLI family factors (Cohen, 2010; Rohatgi et al., 2009); moreover SUFU dissociates from GLI3FL that translocates to the nucleus, where it is converted to a transcriptional activator (GLI3A). When Activated GLIs, the final effectors of the pathway, translocate into the nucleus bind to the GLI1-binding element in GLI1-regulated genes, PTCH, HIP1, D-type cyclins, BMI1, c-MYC and BCL2 which regulate cellular differentiation, proliferation and survival (Shahi et al., 2010; Katoh et al., 2009).

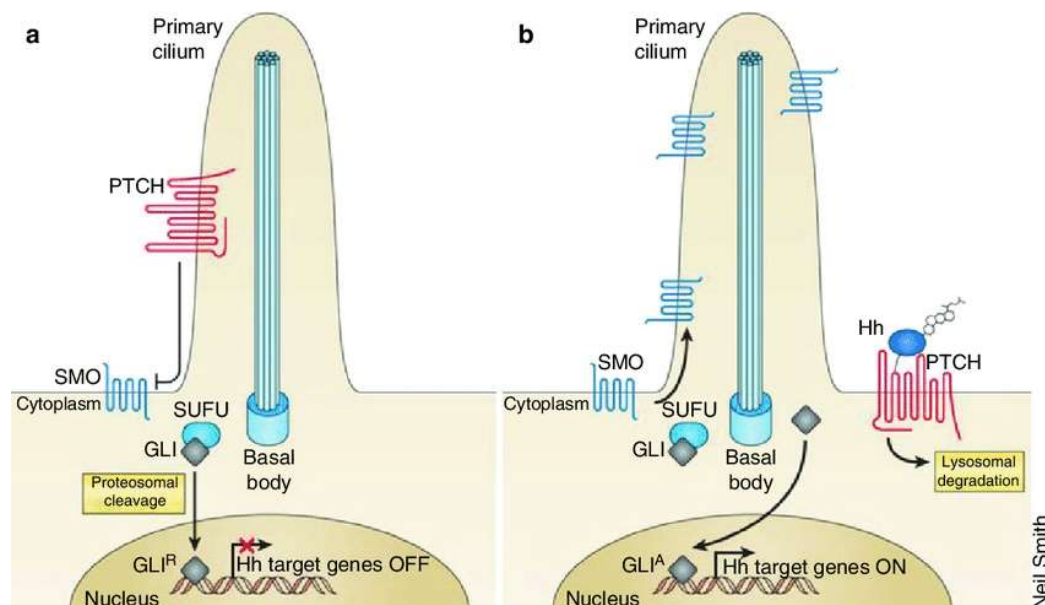


Figure 2. The mammalian Hh signaling pathway: key components and signal transduction. (A) In the absence of Hh ligand, PTCH localizes in the cilia and represses SMO activity by preventing its trafficking and localization to the cilia. GLI transcription factors are sequestered in the cytoplasm by several protein mediators, including suppressor of fused (SUFU). GLI undergoes proteasomal cleavage and the transcription of Hh target genes is repressed. (B) Hh ligand interacts with PTCH; SMO activation induces dissociation between SUFU and GLI factors, that activated translocate into the nucleus and transcribe for Hh target genes.

Components of the Hh pathway are frequently mutated in cancer and various types of Hh pathway activation can occur. Ligand-independent activation is due to inactivating mutations in the negative regulators PTCH1 or SUFU, activating mutations in SMO, or amplification of GLI

activators. Ligand-dependent activation occurs through autocrine, paracrine or reverse paracrine mechanism; in autocrine mechanism tumor cells secrete and respond to HH ligands; in the paracrine pattern tumor cells produce HH ligands, which activate HH pathway in stroma cells; in the reverse-paracrine mechanism stroma cells produce HH ligands, which activate HH pathway in tumor cells.

The discovery of germline loss-of-function mutations in PTCH in patients with nevoid basal cell carcinoma syndrome (NBCCS) correlated Hh pathway activation and cancer. Somatic mutations in PTCH and gain of function mutations in SMO have been identified in basal cell carcinoma (BCC); these mutation have been characterized and functional studies demonstrated that they generate aberrant activation of Hh signaling, promoting tumorigenesis (Xie et al.,1998). In fact in 2012 a SMO antagonist, NVP-LDE225, was approved by the U.S. Food and Drug Administration to treat adult patients with metastatic basal cell carcinoma. (Sekulic et al 2012).

Somatic mutations in PTCH, in SHH and amplification of GLI1 locus have been detected in breast cancer and an aberrant activation of the pathway has been described in breast cancer development and progression (O'Toole et al., 2011; Riku et al., 2015). Several studies demonstrate that HH pathway regulates the promotion of epithelial–stromal interactions (Yauch et al., 2008; Theunissen and de Sauvage, 2009; Angelucci et al., 2012). Emerging data support Hh pathway contribution to cancer cell stemness in TNBC (Habib and O'Shaughnessy, 2016).

Furthermore, the expression of some Hh effectors, such as SMO and GLI1, is significantly increased in TNBC in comparison to non-TNBC (Tao et al., 2011).

1.3 HH pathway and cancer microenvironment

The cancer microenvironment consists of multiple cell populations that participate in crosstalk with tumor cells, regulating tumor growth and progression. The Hh pathway promotes tumor development and progression especially through epithelial-stromal interaction. In ligand-dependent paracrine mechanisms, Hh ligands secreted by tumor cells can positively regulate Hh signaling in the surrounding microenvironment cells that in turn stimulates growth of the tumor. The mechanisms by

which the Hh-stimulated stroma positively regulates tumor cell growth are not fully understood. However, it has been proposed that Hh regulates signaling mediators in the stroma, including insulin-like growth factor (IGF), Wnt, vascular endothelial growth factor (VEGF) and Interleukin-6 (IL-6), creating a favorable cancer microenvironment .

In cancer proliferation and metastasis process new growth in the vascular network is important since new blood vessels allow an adequate supply of oxygen and nutrients and the removal of waste products. The Hedgehog (Hh) pathway has a key role in angiogenesis and vasculogenesis during ontogeny. The ligand, Sonic hedgehog (SHH), plays as an important factor in vascular formation during development (Hochman et al., 2006).

Several recent data suggest the involvement of Hh signaling in tumor-associated angiogenesis: the ligand sonic hedgehog homolog (SHH) can promote angiogenesis in a paracrine manner, stimulating the production of secreted factors (Yamazaki et al., 2008). GLI1, the main transcription factor of the Hh pathway, leads to upregulation of a pro-angiogenic secreted molecule, cysteine-rich angiogenic inducer 61 (CYR61) supporting an increase in tumor vasculature (Harris et al., 2012). It has been demonstrated that GLI1 enhances the production of Neuropilin 2 (NRP2), a VEGFR1 and VEGFR2 co-receptor (Goel et al., 2013). An alternative splicing form of GLI1, 4kDa shorter than full length (truncated GLI1 or tGLI1), enhances the hVEGF-A gene promoter, leading to upregulation of this factor in breast cancer cells (Cao et al., 2012; Carpenter and Lo, 2012).

Recent studies suggest that Hh signaling mediates a crosstalk between breast cancer cells and tumor-infiltrating immune cells (Ann et al., 2018); Hh pathway can promote the production and secretion of some inflammatory mediators such as IL6. IL-6 signaling acts on tumor cells to support cancer cell proliferation, survival, and metastatic dissemination. Moreover, IL-6 can act extrinsically on other cells within the tumor microenvironment to sustain tumor evasion of immune surveillance.

Moreover treatment with systemic Hh inhibitor in BCC causes a reduction of immune-suppressive cells concomitant with an enrichment of cytotoxic immune cells, suggesting a novel role for Hh signaling in disabling anti-tumor immunity (Atsushi et al., 2015)

2. Study purpose

The purpose of this study was to evaluate the complexity of aberrant Hh pathway functions in TNBC and its putative effect in sustaining TNBC microenvironment, suggesting the Hh pathway inhibition as new anti-angiogenic and immune-stimulating therapeutic options in this subtype of tumor.

The study is divided into three tasks:

Task 1) Evaluation of the Hh pathway activation in TNBC cancer cell lines and in TNBC patients;

Task 2) Characterization of the Hh pathway involvement in cancer neo-angiogenesis and Task 3) characterization of the Hh pathway involvement in cancer immune surveillance in order to highlight mechanisms and markers associated to these processes.

3. Materials and Methods

Compounds and cell cultures

NVP-LDE225 and paclitaxel were purchased from Selleck Chemicals (Germany). Bevacizumab was kindly provided by Roche.

For this study, a panel of immortalized (MDA-MB-361, SKBR-3, MCF7, MDA-MB-231, HCC70 and MDA-MB-468, KPL-4, JIMT-1, 4T1) and primary (K90, K79, K193, K197) breast cancer cell lines were used. Besides, some experiments have been performed on endothelial cells such as human umbilical vein endothelial cells (HUVECs) and mouse brain endothelial cell 5 (bEND5). Human breast cancer cell lines MDA-MB-361, SKBR-3, MCF7, MDA-MB-231, HCC70 and MDA-MB-468 were obtained from the American Type Culture Collection. The KPL4 cell line was isolated from the malignant pleural effusion of a breast cancer patient with an inflammatory skin metastasis [1]. The JIMT-1 cell line was established from a pleural metastasis of a 62-year-old breast cancer patient. Cells were routinely grown in RPMI-1640 medium with GlutaMAX supplemented with 10% fetal bovine serum (FBS). SUM-159 and SUM-149 human breast carcinoma cell lines were kindly provided by Dr. Nicola Normanno (Cell Biology and Biotherapy Unit, Istituto Nazionale Tumori “Fondazione Giovanni Pascale”, IRCCS) and maintained in Ham's F12 medium with GlutaMAX (LifeTechnologies) supplemented with 5% FBS and 5 µg/ml insulin. Breast cancer primary cells (K90, K79, K193, K197) were generated by TNBC and nTNBC tumors. Briefly, tissue specimens were collected and processed; primary cultures were generated via standardized operative procedures for banking [2] and cell population expansion, as previously described [3].

Human umbilical vein endothelial cells (HUVECs) were obtained from the American Type Culture Collection; mouse brain endothelial cell 5 (bEND5) were kindly provided by Dr. Mauro Cataldi (Dept. of Neuroscience, University of Naples Federico II). HUVEC cells were grown in F-12K medium, supplemented with 0.1 mg/ml heparin; 0.03-0.05 mg/ml endothelial cell growth supplement (ECGS), FBS. bEND5 were grown in Dulbecco's modified Eagle's medium (DMEM) supplemented with 10% fetal calf serum, 4 mmol/L -glutamine, 1 mmol/L sodium pyruvate, 50 Units/mL penicillin, and 50 µg/mL streptomycin.

Cell lines authentications

Short tandem repeat (STR) profiles of cell lines were obtained using nine highly polymorphic STR loci plus amelogenin (Cell IDTM System, Promega). The amplified fragments were analyzed with the ABI PRISM 3100 Genetic Analyzer. Data analysis was performed by GeneMapper® software, version 4.0. Cell lines authentications was performed by IRCCS Azienda Ospedaliera Universitaria San Martino – Istituto Nazionale per la Ricerca sul Cancro (Genova, Italy). The cells were last tested in August 2015.

Western blot analysis

Total protein extracts obtained from cell cultures or tumor specimens were resolved by 4-15% SDS-PAGE and probed with anti-human and anti mouse GLI11, cyclin D1, PDL1; anti human Smo, VEGFR2, NRP2, pAkt/Akt, pERK/ERK, bcl2 and GAPDH and anti-mouse alfa-tubulin (Cell Signaling Technologies, Beverly, MA, USA; Santa Cruz Biotechnology). Immunoreactive proteins were visualized by enhanced chemiluminescence (Pierce, Rockford, IL, USA).

Capillary tube formation assay

Twenty-four-well plates were coated with 200 µl/well of Matrigel (BD Biosciences, Billerica, MA), allowed to jellify for 30 min at 37°C in a cell culture incubator; HUVEC cells (5×10^4 /well) were plated on top of the Matrigel in TNBC, or nTNBC conditioned growth media, or in RPMI medium supplemented with VEGF-A (100 ng/ml), as a positive control. Cells were observed under an inverted microscope Olympus CKX31 at regular intervals, and pictures were taken after 3 hours.

Co-culture of tumor and endothelial cells

The *in vitro* co-culture model was prepared on Transwell polycarbonate filters (surface area, 0.3 cm²; pore size, 0.3 µm; BD Biosciences Franklin Lakes-USA). bEND5 (2×10^4 /well) were seeded on the

bottom of wells in a 24-multiwell plate, were allowed to adhere for 24 hours, then TNBC or nTNBC cells (5×10^3 /well) were seeded on filters. Tumor and endothelial cells were cultured together for 3 days in DMEM medium.

The percentage of cell density was determined using the 3-(4,5-dimethylthiazol-2-yl)-2,5-diphenyltetrazolium bromide (MTT) assay according to the manufacturer's instructions (Sigma-Aldrich, Milan, Italy).

ELISA assay for determination of VEGF-A, sVEGFR2, and THBS1 concentrations

Anti-human VEGF polyclonal antibody (R&D Systems, Minneapolis, MN, USA), diluted at $1 \mu\text{g/ml}$ in PBS pH 7.5, was used to coat a 96-well plate, $100 \mu\text{l/well}$, overnight at 4°C . Washings, dilutions of standards (recombinant hVEGF) and samples (conditioned media from tumor cells or sera from sacrificed mice), biotinylation, and mixtures with preformed avidin and biotinylated HRP macromolecular complex (Vectastain kit) were performed as previously described (D'Amato et al., 2014). Absorbance was measured at 490 nm on a microplate reader (Bio-Rad, Hercules, CA, USA). VEGF concentrations were determined by interpolation of the standard curve using linear regression analysis.

sVEGFR2 and THBS1 concentrations on conditioned media from tumor cells or sera from sacrificed mice have been measured by using sVEGFR2 and THBS1 Quantikine ELISA kits (R&D Systems, Minneapolis MN, USA).

Multiplexed immunoassay

The quantitative analysis of secreted cytokines and chemokines in conditioned media (CM) of MDA-MB-231, SUM-159, SUM-149, HCC70 and MDA-MB-468 in presence or absence of NVP-LDE225 ($2.5 \mu\text{M}$), was performed by the Bio-Plex multiplex system (Bio-Rad, Milan, Italy), based on xMAP technology that uses magnetic beads coated with specific antibodies raised against target analytes. Briefly, microspheres are internally labeled with red and infrared fluorophores. Each bead is bound

to a specific antibody, thus allowing the simultaneous detection of multiple analytes within one sample. Following reaction of coupled beads with target analytes, a biotinylated antibody is added for the detection, which is then finalized by adding phycoerythrin-conjugated streptavidin. All steps were performed according to manufacturer's instructions for determining the concentration of sEGFR, FGF-basic, Follistatin, G-CSF, HGF, sHER-2/neu, sIL-6R α , Leptin, PECAM-1, PDGF-AB/BB, Prolactin, SCF, sTIE-2, THBS1, sVEGFR-1, sVEGFR-2. Data were acquired using a Bio-Plex MAGPIX Multiplex Reader system equipped with a Bio-Plex Manager software v 6.1 (BioRad). All washing steps were performed on the Bio-Plex magnetic wash station (BioRad). Measurements were performed on CM samples (50 μ L) using the Bio-Plex Pro human cancer biomarker panel 1 (Cat. N $^{\circ}$ 171AC500M, BioRad) according to the manufacturer's protocol. An aliquot of RPMI /F12/ (50 μ L) was also analyzed as negative control. Standard curves optimization and the calculation of analyte concentrations were performed by using the Bio-Plex Manager software. Data were expressed as mean \pm SD. A two-tailed t-test was used to test the significance between conditions by using the GraphPad Prism software v 5.0 (La Jolla, CA USA).

MTT survival assay

Cells (10^4 cells/well) were grown in 24-well plates and exposed for 72 hours to increasing doses of NVP LDE 225 or GANT61. The percentage of cell survival was determined by using the 3-(4,5-dimethylthiazol-2-yl)-2,5-diphenyltetrazolium bromide assay (MTT). The half-maximal inhibitory concentration (IC₅₀) for each drug was calculated by GraphPad Prism 5.0 software, normalizing the response between 0 and 100%.

RNA extraction and analysis

Total RNA was isolated from cells using TRIZOL reagent (Invitrogen). 2 μ g of total RNA was reverse transcribed using 100 ng of random hexamer primers and Super Script III Reverse Transcriptase

(Invitrogen). Real Time RT-PCR (qRT-PCR) experiments were performed using the CFX96 Real-Time PCR Detection System (Bio-Rad); PCR reactions were in a final volume of 15 μ l, using 5 ng of cDNA and iQ SYBR Green Supermix 2X (Bio-Rad). Reagents and enzymes were employed according to manufacturer's instructions. PCR cycling profile consisted of a cycle at 95° C for 10 min and 40 two-step cycles at 95° C for 10 sec and at 60° C for 60 sec. Primers were chosen using Primer3 software (<http://bioinfo.ut.ee/primer3/>) and designed to span exon/exon borders; their sequences are listed in the Table 1. Three different RNA preparations were tested for each sample, and each reaction was run in triplicate.

Table 1. Sequences of primers used for Real Time RT-PCR.

GENE	FORWARD SEQUENCE	REVERSE SEQUENCE
sVEGFR2	TGGTCAGGCAGCTCACAGT	TCACTCTGAGTCTTCTACAAGG
VEGFR2	TTACAGCTTCCAAGTGGCTAAGG	TTAACCACGTTCTTCTCCGATAA
THBS1	CAATGCCACAGTTCCTGATG	TGGAGACCAGCCATCGTC
PDL1	AAACAATTAGACCTGGCTG	TCTTACCACTCAGGACTTG
G6PD	GAGCCAGATGCACTTCGTG	GGGCTTCTCCAGCTCAATC
β -ACTIN	GAAATCGTGCGTGACATTAA	AAGGAAGGCTGGAAGAGTG

RNA interference

Smart siRNA pool against all isoforms of GLI1 was purchased from GE Healthcare Dharmacon. A nonsense sequence was used as negative control. For siRNA validation, cells were transfected with GLI1 siRNAs (50 nmol/L) using DharmaFECT 1 Transfection Reagent in DMEM (Dharmacon); 24

and 48 hours after transfection, western blot analysis for GLI1 and VEGFR2 expression was performed.

Cell transfection with GLI1 expression vectors

MDA-MB-231 and HCC70 cells were cultured in RPMI medium supplemented with 10% FBS, 100 U/ml penicillin and 100 µg/ml streptomycin (all from Invitrogen) and grown at 37° C in a humidified atmosphere containing 5% CO₂. For transfection, 5µg of either pCMV6-GFP GLI1, pCMV6-GFP tGLI1, pCMV6-GFP empty vector plasmid (Origene) were added together with lipofectamine 2000 Reagent (Invitrogen), following the manufacturer's instructions.

Luciferase Assay

Luciferase assay was performed by using the Dual-Luciferase Assay system (Promega) following the manufacturer's protocol. A total of 5×10^5 MDA-MB-468 cells were plated 24 hours before transfection in a 24-wells multiwell plate. The GLI-Luc reporter plasmid (Promega) was transfected together with pRL-TK, encoding the Renilla luciferase (Promega), in triplicate, using lipofectamine 2000 Reagent (Invitrogen) with the luciferase reporter. Twenty-four hours after transfection, cells were treated with NVP-LDE225 5µM. Luciferase activity was determined 48 h after transfection by using a BioTek Microplate Luminescence Reader (BioTek, Winooski, VT, USA).

ChIP assay

The chromatin immunoprecipitation (ChIP) assay was performed in MDA-MB-468 cells using ChIP Assay Kit (Millipore) following the manufacturer's instructions. Crosslinking of the target proteins to the chromatin DNA with formaldehyde and breaking of the chromatin DNA into fragments (200-1200 bp) were performed. Immunoprecipitation (IP) of the protein-DNA complex was performed using a GLI1 antibody (Santa Cruz Biotechnology- Heidelberg, Germany). The DNA in IP products

was amplified by RT-PCR with ChIP assay primers specific for the VEGFR2 and PDL1 promoters. Results were reported as fold changes relative to input.

Orthotopic breast xenograft model in nude mice

Five-week-old Balb/cAnNCrI BR athymic (nu⁺/nu⁺) mice (Charles River Laboratories, Milan, Italy) maintained in accordance with institutional guidelines of the University of Naples Animal Care Committee and in accordance with the Declaration of Helsinki were injected into the fourth mammary fat pad with MDA-MB-468 cells (10⁷ cells per mice) resuspended in 200 µl of Matrigel (BD Biosciences, Billerica, MA). Seven days after the tumor cell injection, tumor-bearing mice were randomly assigned (n: 10 per group) to receive the following: NVP-LDE225 20 mg/kg *per os* every day for 4 weeks; bevacizumab 5 mg/kg intravenously (i.v.), twice a week for 4 weeks, or a combination of these agents with paclitaxel i.v. 10 mg/kg once a week for 4 weeks. Tumor diameter was assessed with a vernier caliper, and tumor volume (cm³) was measured using the formula $\pi/6 \times (\text{larger diameter}) \times (\text{smaller diameter})^2$. Mice were killed when the tumor reached 2 cm³, the maximum size allowed by the ethics committee.

TMA building

A breast Tissue Micro Array (TMA) was constructed using 237 samples of TNBC collected from 2003 to 2013 from the Pathology Unit of the Istituto Nazionale Tumori of Naples. Informed consent was obtained from all patients. All tumors and controls were reviewed by two experienced pathologists (M.D.B./G.B.) according to WHO classification criteria, using standard tissue sections and appropriate immunohistochemical slides. Discrepancies between two pathologists from the same case were resolved in a joint analysis of the cases. Moreover, all specimens were characterized for all routinely diagnostic immunophenotypic parameters (ER, PGR, HER2 and Ki67). TMA was built using the most representative areas from each single case with one replicate. Tissue cylinders with a diameter of 1 mm were punched from morphologically representative tissue areas of each 'donor'

tissue block and brought into one recipient paraffin block (3 × 2.5 cm) using a semi-automated tissue arrayer (Galileo TMA).

Immunohistochemical analysis

For immunohistochemical analysis on mice tumor specimens, excised tumors were split into two halves and immediately fixed in 10% buffered formalin solution. Twelve hours later, tissues were embedded in paraffin in an automated tissue processor. Sections (4-5 μm) were then cut with a serial microtome and mounted on adhesive poly-L-lysine-coated slides. After being dried in an oven at 40° C for 8 hours, the slides were processed for immunohistochemistry (IHC) in a semi-automated machine (Menarini Bond Max, Menarini, Florence, Italy) with the following antibodies: CD31, GLI1, NRP2, VEGFR2 and PDL1 (Novocastra, Newcastle, United Kingdom).

Immunohistochemical staining on TMA slides was done from formalin-fixed, paraffin embedded tissues to evaluate the expression of GLI1, VEGFR2 and PDL1 markers in human tumors. For PDL1 presence or absence of staining was evaluated (positive or negative expression). There are not standardized criteria for VEGFR2 and Gli1 markers staining evaluation. The staining intensity was graded as follows: 0, negative; 1, weak; 2, moderate; and 3, intense; the proportion was graded according to the percentage of positive cells as follows: 0, negative; 1, 1-14%; 2, ≥15%. The intensity score and proportion score were multiplied in order to generate an immunoreactive score (IS). IS 0 defines negative expression, IS ranging between 1 and 3 defines moderate expression and IS greater than 3 high expression.

4. Results

4.1 Task 1:

GLI1 is frequently overexpressed in TNBC primary and immortalized cell lines.

We investigated the expression of the main Hh pathway transducers in ten human breast cancer cell lines, five ER/PgR+ and/or HER2+ (nTNBC) and five ER/PgR- and HER2- (TNBC). None of the cell lines used display mutations in the major Hh signaling components; the molecular features of the selected cell lines are depicted in Table 2.

Table 2. Clinicopathological features of the human breast cancer cell lines included in the study.

Cell line	Subtype ¹⁻²⁻³⁻⁴	Source ²⁻³⁻⁴⁻⁵	Tumor type ⁵	TNBC subtype ⁶
MDA-MB-361*	L	BR	Met AC	
SKBR3*	HER2 positive	PE	AC	
JIMT1*	HER2 positive	PE	DC	
MCF7*	L	PE	Met AC	
KPL4*	HER2 positive	PE	Met C	
MDA-MB-231*	B	PE	Met AC	MSL
SUM-159*	B	PT	ANC	MSL
SUM-149*	B	PE	INF	BL2
HCC70*	A	PT	DC	BL2
MDA-MB-468*	A	PE	Met AC	BL1

A=basal A subtype; AC= adenocarcinoma; ANC= anaplastic carcinoma; B=basal B subtype; BL1=basal-like1; BL2=basal-like2; BR= brain; DC= ductal carcinoma; INF= inflammatory ductal carcinoma; L=luminal subtype; Met AC= metastatic adenocarcinoma; Met C= metastatic carcinoma; MSL= mesenchymal-stem-like; PE= pleural effusion; PT=primarytumor. * No PATCH, SHH, SMO and GLI1 mutations reported in COSMIC and ATCC databases.

1. Neve RM, Chin K, Fridlyand J, Yeh J, Baehner FL, Fevr T et al. A collection of breast cancer cell lines for the study of functionally distinct cancer subtypes. *Cancer Cell*. 2006;10(6):515-27. 2. Kristina Subik, Jin-Feng Lee, Laurie Baxter, Tamera Strzepak, Dawn Costello, Patti Crowley et al. The Expression Patterns of ER, PR, HER2, CK5/6, EGFR, Ki-67 and AR by Immunohistochemical Analysis in Breast Cancer Cell Lines. *Breast Cancer (Auckl)*. 2010; 4: 35–41. 3. Tanner M, Kapanen AI, Junttila T, Raheem O, Grenman S, Elo J et al. Characterization of a novel cell line established from a patient with Herceptin-resistant breast cancer. *Mol Cancer Ther*.2004;3(12):1585-92. 4. Kurebayashi J, Otsuki T, Tang CK, Kurosumi M, Yamamoto S, Tanaka K et al. Isolation and characterization of a new human breast cancer cell line, KPL-4, expressing the Erb B family receptors and interleukin-6. *Br J Cancer*. 1999; 79(5-6):707-17. 5. Kao J, Salari K, Bocanegra M, Choi YL, Girard L, Gandhi J et al. Molecular profiling of breast cancer cell lines defines relevant tumor models and provides a resource for cancer gene discovery. *PLoS One*. 2009; 3;4(7):e6146. 6. Lehmann BD, Bauer JA, Chen X, Sanders ME, Chakravarthy AB, Shyr Y, Pietsenpol JA. Identification of human triple-negative breast cancer subtypes and preclinical models for selection of targeted therapies. *J Clin Invest*. 2011;121(7):2750-67.

The expression of SMO and mostly GLI1 was higher in TNBC cell lines (Fig. 3A). Similar results have been obtained in primary breast cancer cell lines, generated from two ER+ breast cancer patients

and two triple negative ones: overexpression of GLI1, as well as of its truncated form tGLI1, was also evident in these models (Fig. 3B). The HH pathway ligands Desert Hedgehog (DHH), Indian Hedgehog (IHH) and Sonic Hedgehog (SHH) showed comparable expression in all the analyzed cancer cell lines (Fig. 3C).

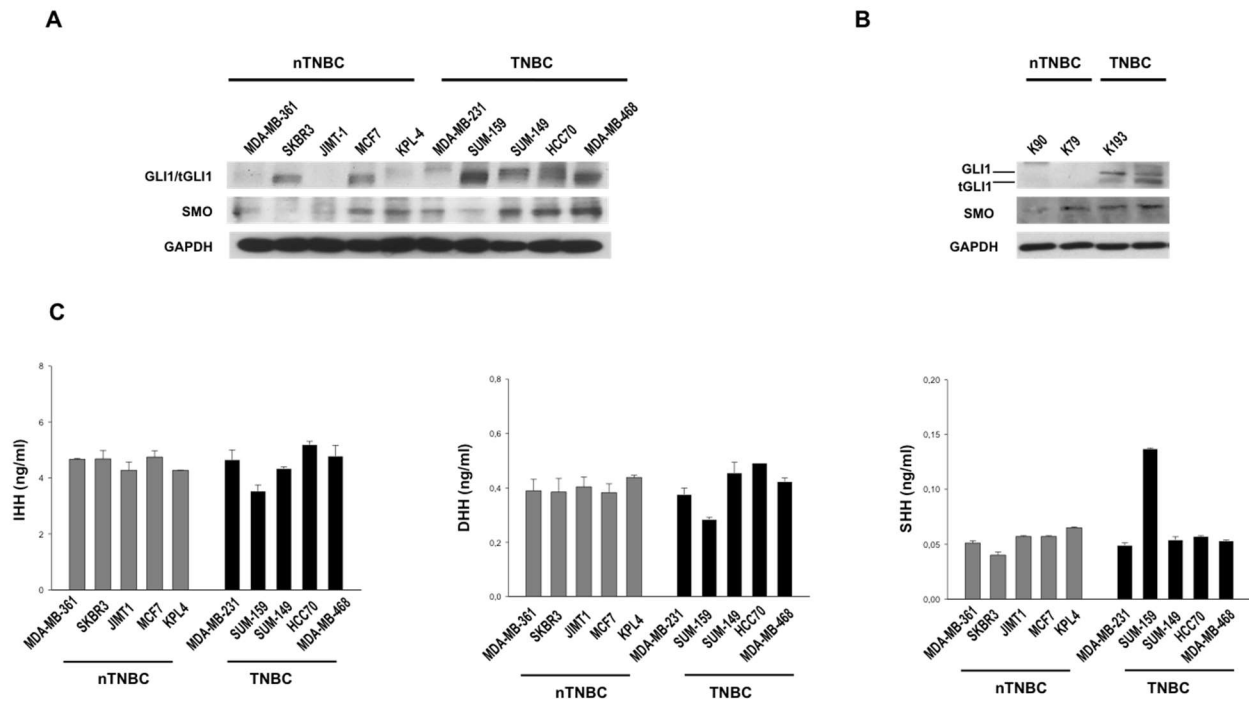


Figure 3. GLI1 is frequently overexpressed in TNBC primary and immortalized cell lines.

(A, B) Western blot analysis of protein expression in a panel of (A) nTNBC or TNBC immortalized cell lines, and (B) nTNBC or TNBC primary cell lines. (C) HH ligands expression in conditioned media of immortalized cells. ELISA assay for the determination of IHH, DHH and SHH concentrations (ng/ml) in conditioned media from nTNBC or TNBC immortalized cells. Data represent the mean (\pm SD) of three independent experiments, each performed in triplicate.

GLI1 expression in TNBC patients

To evaluate the relevance of Hh pathway activation in triple negative breast cancer (TNBC), we analyzed a TNBC TMA by immunohistochemistry. The patient cohort included 237 TNBC samples

of breast cancers; the age of patients ranged from 24 to 93 years (average age = 57 years). Clinical-pathological characteristics and follow-up data of TNBC patients are depicted in Table 3.

Table 3. Clinical-pathological characteristics and follow-up data of TNBC patients included in the TMA

Grade		Metastatic lymph nodes (LNM)	
grade I-II	11.8%	positive	34.0%
grade III	82.8%	negative	46.6%
not available	5.4%	not available	19.4%
Tumor size		Ki67 expression	
< 2 cm	42.9%	high	78.2%
2 – 5 cm	43.3%	low	17.6%
> 5 cm	8.4%	not available	4.2%
not available	5.4%		
Distant metastases			
positive	17.6%		
negative	55.0%		
not available	27.4%		

The evaluated cases were 200/237. Tumor samples were classified based on the Immunoreactive Score (IS, see Methods section). As shown in 24/200 cases (12.0%) there was a high GLI1 expression

(IS>3), in 53/200 cases (26.5%) there was a moderate expression ($1 < IS < 3$) and in 123/200 cases (61.5%) there was no GLI1 expression with IS equal to 0 (Fig. 4A).

4.2 Task2:

GLI1 expression correlates with VEGFR2 in TNBC patients

VEGFR2 expression was assessed in all samples evaluated for GLI1 expression: as shown in figure 4B, 9/200 TNBC samples (4.5%) showed high expression for VEGFR2 (IS>3), 20/200 (10.0%) showed moderate expression ($1 < IS < 3$), while 171/200 cases (85.5%) resulted negative (IS=0). Considering the 20 samples with VEGFR2 IS ranging from 1 to 3, 7/20 cases (35.0%) were negative for GLI1 expression (IS=0), 9/20 (45.0 %) showed moderate expression for GLI1 ($1 < IS < 3$) and 4/20 (20.0 %) showed GLI1 high expression (IS>3). Notably, among the 9 samples showing VEGFR2 IS>3, all showed IS>3 also for GLI1 (100.0 %). Statistical analysis demonstrated a direct significant association between VEGFR2 and GLI1 expression in TNBC patients ($P = 0.000$, R Pearson = 0.489), as shown in Table 4.

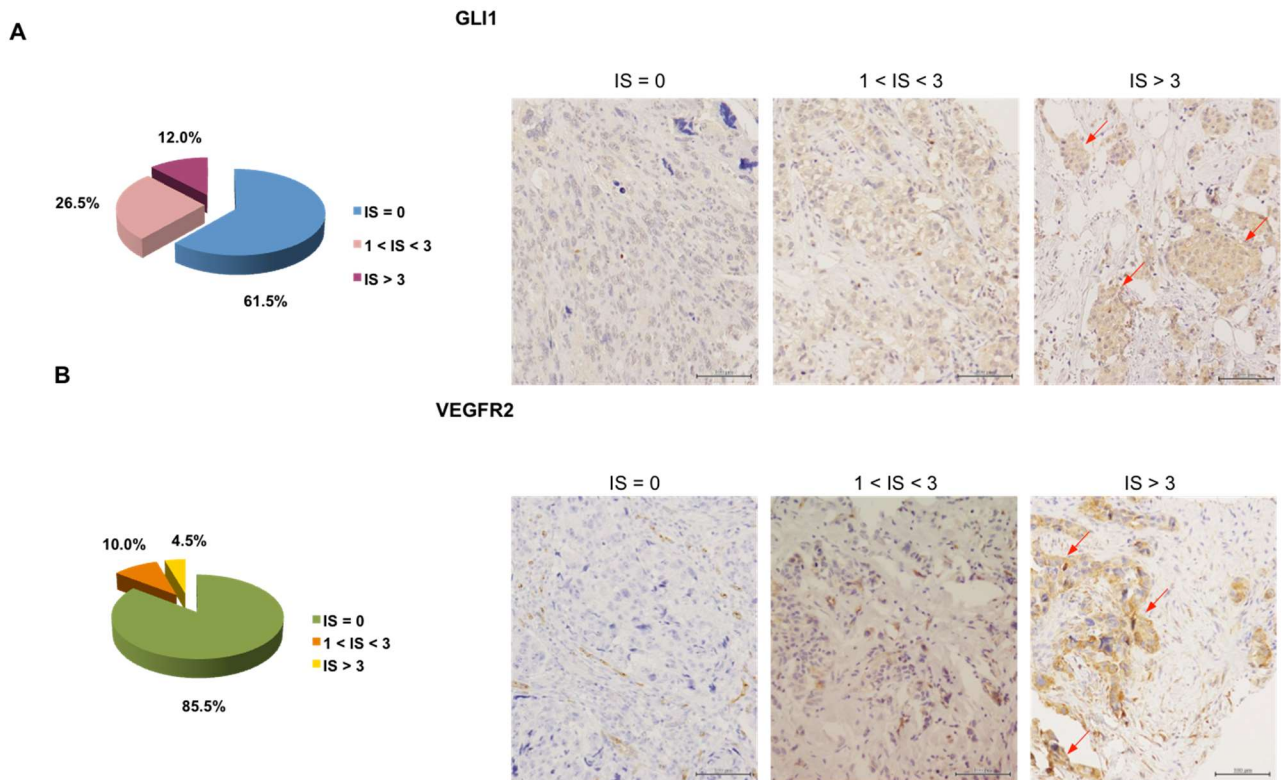


Figure 4. GLI1 expression correlates with VEGFR2 in TNBC patients.

(A) *Left*, pie chart representing the percentage of samples included in the TMA that show IS equal to 0, $1 < IS < 3$ and $IS > 3$ for GLI1 expression, respectively. *Right*, immunohistochemical images representing GLI1 negative ($IS = 0$) or positive tumors with moderate ($1 < IS < 3$) or high ($IS > 3$) expression levels, respectively (20X magnification). The red arrows indicate representative highly GLI1 positive signal. (B) *Left*, pie chart representing the percentage of samples included in the TMA that show Immunoreactive score (IS) equal to 0, $1 < IS < 3$ and $IS > 3$ for VEGFR2 expression. *Right*, immunohistochemical images representing VEGFR2 negative ($IS = 0$) or positive tumors with moderate ($1 < IS < 3$) and high ($IS > 3$) expression levels, respectively. Endothelial cells positivity represents internal control (20X magnification). The red arrows indicate representative highly VEGFR2 positive signal.

Table 4. Correlation between GLI1 and VEGFR2 expression in TNBC patients.

		GLI1			<i>P value</i>	<i>R Pearson</i>
		IS = 0	1 < IS < 3	IS > 3		
VEGFR2	IS = 0	116	44	11	0.000	0.489
	1 < IS < 3	7/20 (35.0%)	9/20 (45.0%)	4/20 (20.0%)		
	IS > 3	0/9 (0.0%)	0/9 (0.0%)	9/9 (100.0%)		

Hh pathway regulates the production of pro- and anti-angiogenic secreted factors.

Interestingly, the triple-negative condition of cell models, used in the study, seems to influence tumor angiogenesis, as demonstrated by capillary tube formation assay performed with HUVEC cells grown in conditioned media from cultured MDA-MB-361 (nTNBC) or MDA-MB-468 (TNBC) cells. Medium from TNBC cells strongly promoted the endothelial cells ability to form capillary structures; the stimulation was comparable to that obtained by treatment with VEGF-A (Fig. 5A). In order to better evaluate the effect of tumor cells on endothelial cell proliferation, co-cultures of mouse brain endothelial cells bEND5 and breast cancer cell lines were performed. As shown in figure 5B, TNBC cells promoted bEND5 proliferation in a stronger manner than nTNBC; consistent with this finding, TNBC cell lines (Fig. 5C), as well as TNBC primary cells (Fig. 5D) secreted higher levels of VEGF-A compared to nTNBC ones.

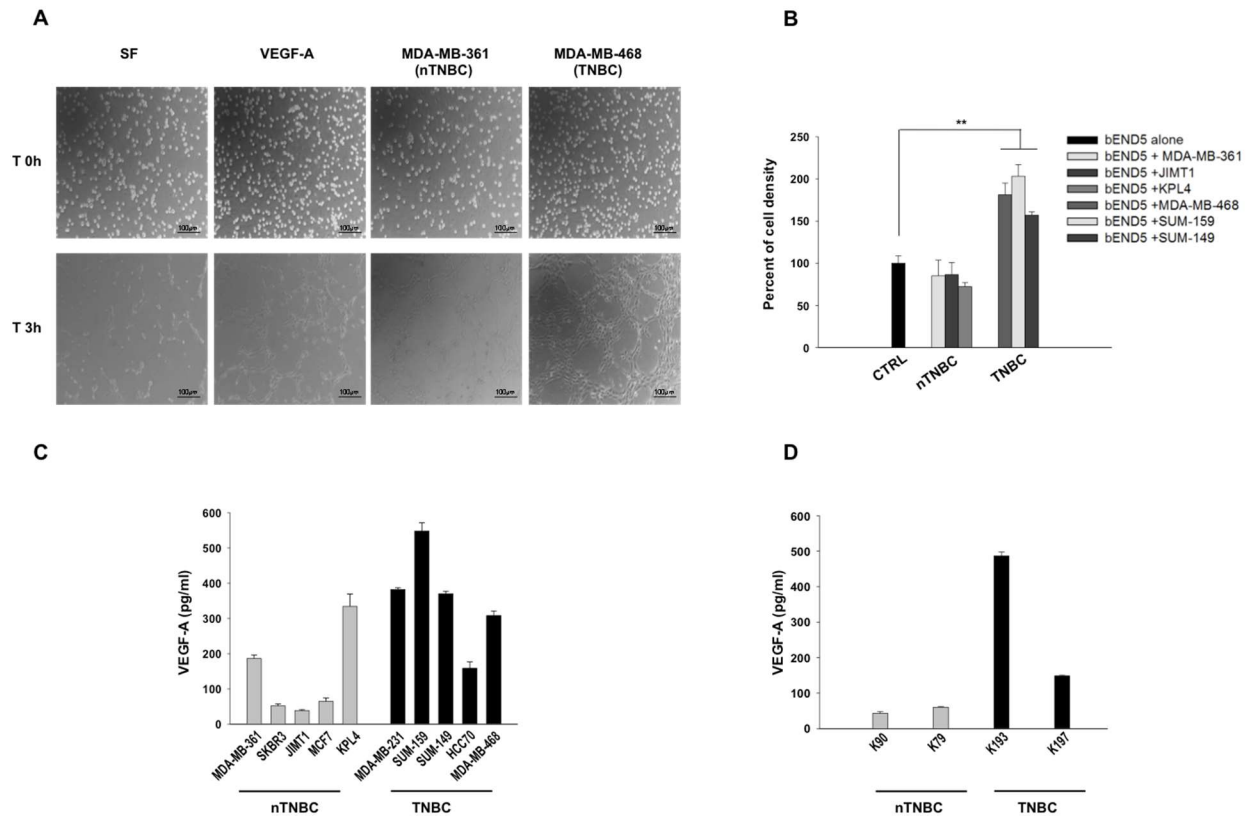


Figure 5. Hh pathway and in vitro angiogenesis. (A) Capillary tubes formation assay on HUVEC cells grown on Matrigel in: RPMI serum free medium; RPMI serum free medium supplemented with VEGF-A (100 ng/ml); conditioned growth media from nTNBC (MDA-MB-361) or TNBC (MDA-MB-468). Cells were observed under an inverted microscope, and pictures were taken at T0 hours and after 3 hours. Scale bars, 100 μ m. (B) Percent of cell density of bEND5 endothelial cells co-cultured with nTNBC or TNBC cells for 3 days, as measured by MTT assay. Data represent the mean (\pm SD) of three independent experiments, each performed in triplicate. (C, D) ELISA assay for determination of VEGF-A concentrations (pg/ml) in conditioned media from (C) nTNBC or TNBC immortalized cells, or (D) primary cells. Data represent the mean (\pm SD) of three independent experiments, each performed in triplicate.

To investigate the putative role of Hh activation in TNBC dependent regulation of tumor angiogenesis, the effects of Hh pathway inhibition on angiogenesis have been compared with those obtained with bevacizumab, a humanized anti-VEGF monoclonal antibody (mAb) (Ferrara et al., 2004). To this aim, we used the selective SMO antagonist NVP-LDE225, a clinically approved drug for the treatment of basal cell carcinoma (BCC) (Sekulic et al., 2012; Rudin, 2012). A capillary tube formation assay was performed using HUVEC cells grown in the conditioned medium of MDA-MB-

468 treated with NVP-LDE225 or bevacizumab: NVP-LDE225 treatment discouraged endothelial cells organization in capillary tubes in a more effective manner than bevacizumab (Fig. 6A). Conversely, bevacizumab determined a reduced presence of secreted VEGFA in culture medium compared to NVP-LDE225 treatment, as shown in figure 6B.

The paracrine effect of Hh pathway inhibition by NVP-LDE225 on tumor microenvironment was also evaluated *in vivo*, in Balb/C nude mice orthotopically xenografted with MDA-MB-468 cells and treated with NVP-LDE225 or bevacizumab. Two weeks after starting treatments, mice were sacrificed, and the expression of the angiogenic marker CD31 on tumor tissue was evaluated through immunofluorescence analysis (figure 6C). NVP-LDE225 appears to be more effective in inhibiting angiogenesis than bevacizumab. Based on these data, we hypothesized that Hh inhibition could lead to dysregulation of some uncharacterized secreted factors, able to regulate tumor angiogenesis. Therefore, a multiplex ELISA assay for 16 secreted factors was conducted on TNBC media upon treatment of TNBC cultured cells with NVP-LDE225. Levels of soluble VEGFR2 (sVEGFR2) and thrombospondin1 (THBS1) significantly increased in TNBC cell supernatants after NVP-LDE225 treatment (Fig. 6D, 6E); sVEGFR2 and THBS1 mRNA levels were augmented as well (Fig. 6F, 6G). These data have been confirmed by ELISA assays specific for each analyte (data not shown). These findings are of interest since sVEGFR2 and THBS1 are known as two endogenous angiogenesis and lymphangiogenesis inhibitors (Nyberg et al., 2005).

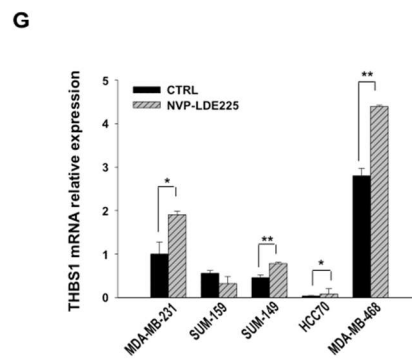
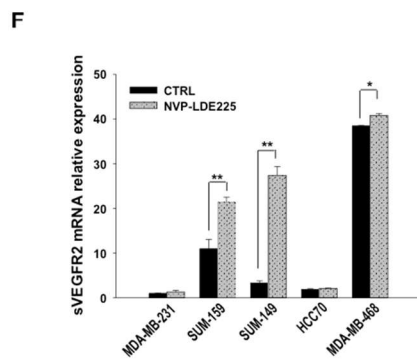
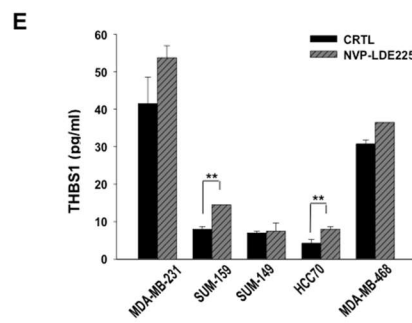
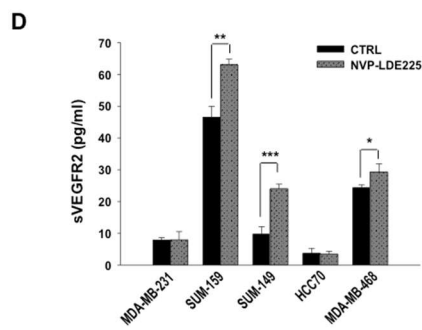
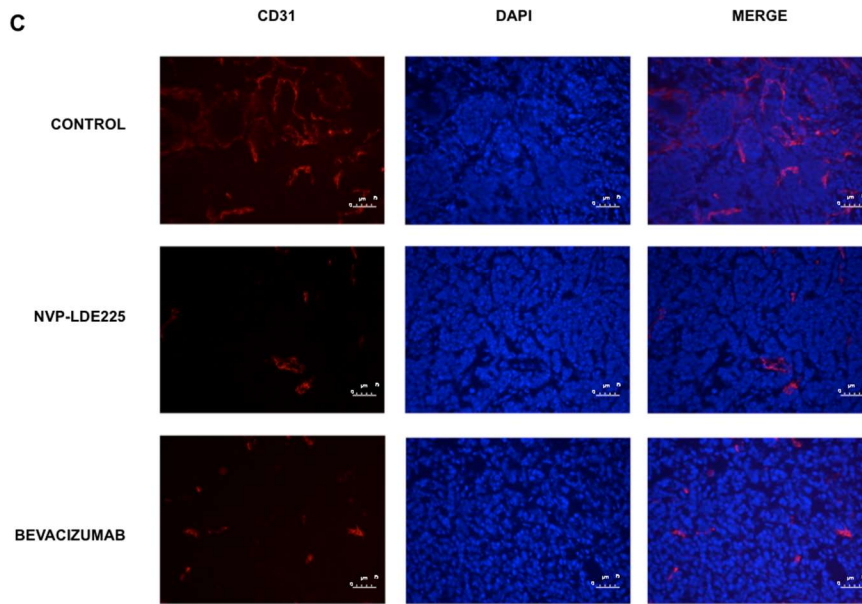
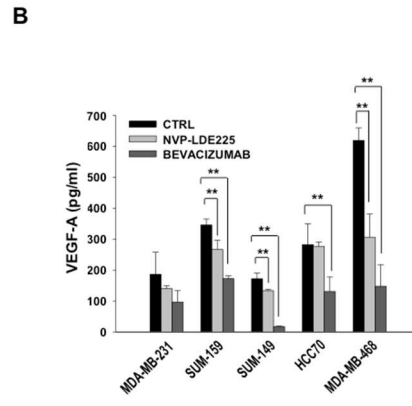
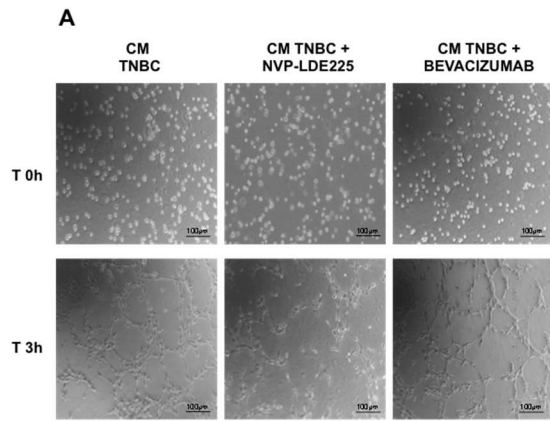


Figure 6. Hh pathway regulates the production of pro- and anti-angiogenic secreted factors.

(A) Capillary tubes formation assay on HUVEC cells grown on Matrigel in presence of conditioned growth media of TNBC (MDA-MB-468) cells treated with NVP-LDE225 (2.5 μ M) or bevacizumab (1 μ M). Cells were observed under an inverted microscope, and pictures were taken at T0 hours and after 3 hours. Scale bars, 100 μ m. (B) Quantitative analysis of VEGF-A in conditioned media (CM) of MDA-MB-231, SUM-159, SUM-149, HCC70 and MDA-MB-468 cells treated with NVP-LDE225 (2.5 μ M) or bevacizumab (1 μ M). (C) Expression of CD31 protein (red) in tumor tissues from nude mice xenografted with TNBC tumors, as measured by immunofluorescence analysis on day 21, after two weeks of treatment with NVP-LDE225 or bevacizumab. Nuclei are stained in blue (DAPI). Merged row images show overlapping of CD31 and DAPI signals. Scale bars, 75 μ m.

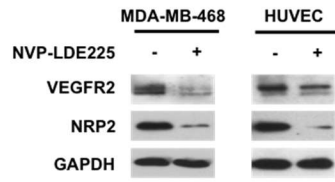
(D, E) Quantitative analysis of (D) sVEGFR2 and (E) THBS1 in CM of MDA-MB-231, SUM-159, SUM-149, HCC70 and MDA-MB-468 cells treated with NVP-LDE225 (2.5 μ M), as performed by using a multiplexed immunoassay. (F, G) Relative expression of (F) sVEGFR2 and (G) THBS1 mRNA in MDA-MB-231, SUM-159, SUM-149, HCC70 and MDA-MB-468 treated with NVP-LDE225 (2.5 μ M), as performed by Real Time RT-PCR (qRT-PCR) analysis. Data were calculated with mean cycle threshold (CT) values, normalized to endogenous control. Data represent the mean (\pm SD) of three independent experiments, each performed in triplicate. Bars, SDs. Asterisks indicate statistical significance, as determined by the Student t-test (* P < 0.05, ** P < 0.01, *** P < 0.001).

GLI1 regulates VEGFR2 expression.

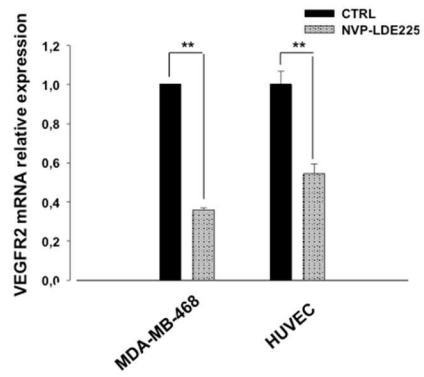
To investigate the capability of Hh pathway to modulate components of the angiogenic machinery, expression of VEGFR2 has been measured: after treatment with NVP-LDE225 a reduction of protein and mRNA levels was observed in both MDA-MB-468 and HUVEC cells (Fig.7A, 7B), an event paired with a simultaneous reduction of NRP2, as already known (Goel et al., 2013). Therefore, we hypothesized that Hh could be involved in the transcriptional modulation of the VEGFR2 receptor, eventually mediated by GLI1. To address this issue, GLI1/tGLI1 silencing was performed in MDA-MB-468 and HUVEC cells using a siRNA pool for all GLI1 forms. As depicted in figure 7C, GLI1 silencing caused down-regulation of VEGFR2 protein expression. Then GLI1 and tGLI1 overexpressions were performed in MDA-MB-231, a TNBC cell line with a low endogenous expression of GLI1. The levels of VEGFR2 protein augmented when tGLI1 was overexpressed, as

shown in figure 7D. A bioinformatic analysis looking for a known GLI1/tGLI1-binding site (Kinzler and Vogelstein, 1990) revealed two putative sequences within ≈ 500 bp upstream of VEGFR2 transcription start site (Fig. 7E). Therefore, we carried out a luciferase reporter assay. As shown in figure 7F, VEGFR2 gene promoter is activated in GLI1 overexpressing MDA-MB-468 cells, and NVP-LDE225 treatment significantly abrogates its activity (P value < 0.001). To further validate the functional GLI1/VEGFR2 promoter interaction, we performed a chromatin immunoprecipitation analysis following by PCR amplification of four different regions (P1 to P4) of VEGFR2 gene promoter (Fig. 7E). We found that tGLI1 binds the VEGFR2 promoter, especially in the P3 region, confirming that tGLI1 transcriptionally enhances VEGFR2 (Fig. 7G). The graphical representation of tGLI1 binding site on VEGFR2 promoter region is shown in the figure 7H. The down-regulation of VEGFR2 observed upon NVP-LDE225 could be related to an interference with GLI1 intracellular localization, since NVP-LDE225 can reduce nuclear translocation of GLI1 and to increase its cytoplasmic retention, as demonstrated by western blot and immunofluorescence assays (Fig. 8A, 8B).

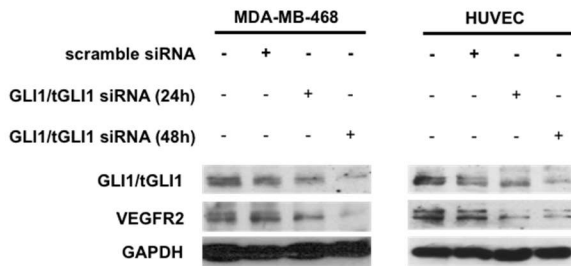
A



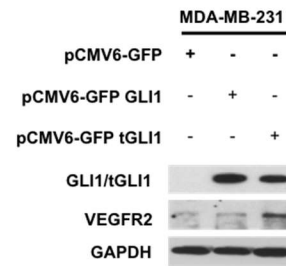
B



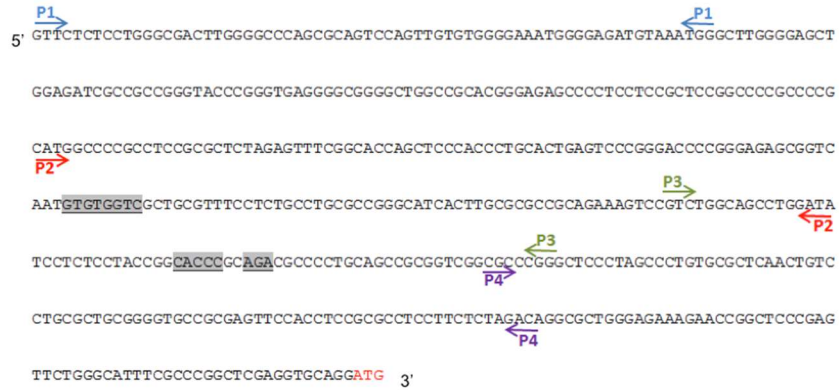
C



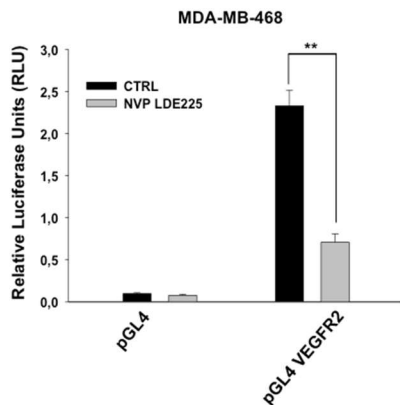
D



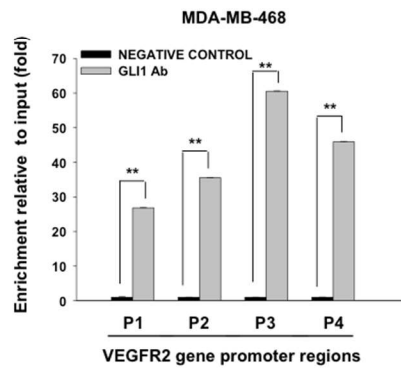
E



F



G



H

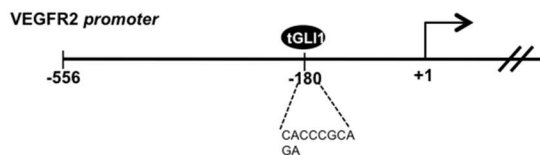


Figure 7. GLI1 regulates VEGFR2 expression.

(A) Western blot analysis of protein expression in MDA-MB-468 and HUVEC cells treated with NVP-LDE225 (2.5 μ M). (B) Relative expression of sVEGFR2 mRNA in MDA-MB-468 and HUVEC cells treated with NVP-LDE225 (2.5 μ M), as performed by Real Time RT-PCR (qRT-PCR) analysis. Data were calculated with mean cycle threshold (CT) values, normalised to endogenous control. Data represent the mean (\pm SD) of three independent experiments, each performed in triplicate. (C) Western blot analysis of protein expression in MDA-MB-468 and HUVEC cells, 24 and 48 hours after transfection with scramble or GLI1 siRNA pool (50 nmol/L) using DharmaFECT 1 Transfection Reagent in DMEM. (D) Western blot analysis of protein expression in MDA-MB-231 cells, 24 hours after transfection with either pCMV6-GFP empty vector, pCMV6-GFP GLI1, or pCMV6-GFP tGLI1 plasmids using lipofectamine 2000 in DMEM. (E) Putative GLI1/tGLI1-binding sites within VEGFR2 gene promoter: two putative GLI1/tGLI1-binding sites upstream of VEGFR2 transcription start site (ATG, in red) are highlighted in grey. Sequence of VEGFR2 gene promoter is represented, highlighting the four regions (P1 to P4) used for ChIP assay. (F) Relative luciferase units in MDA-MB-468 cells transfected with the empty pGL4 plasmid or the pGL4 plasmid containing 500 bp fragment of VEGFR2 promoter, and treated with NVP-LDE225 5 μ M 24h after transfection. Luciferase activity was determined 48h after transfection. Results were the average of three independent experiments. (G) Chromatin immunoprecipitation (ChIP) assay in MDA-MB-468 cells by using a GLI1 antibody and primers specific for the VEGFR2 promoter. Results were reported as fold change compared to negative control (no antibody); results were the average of three independent experiments. Bars, SDs. Asterisks indicate statistical significance, as determined by the Student t-test (** $P < 0.01$). (H) Graphical representation of VEGFR2 proximal promoter region, containing the binding site of tGLI1 indicated by oval.

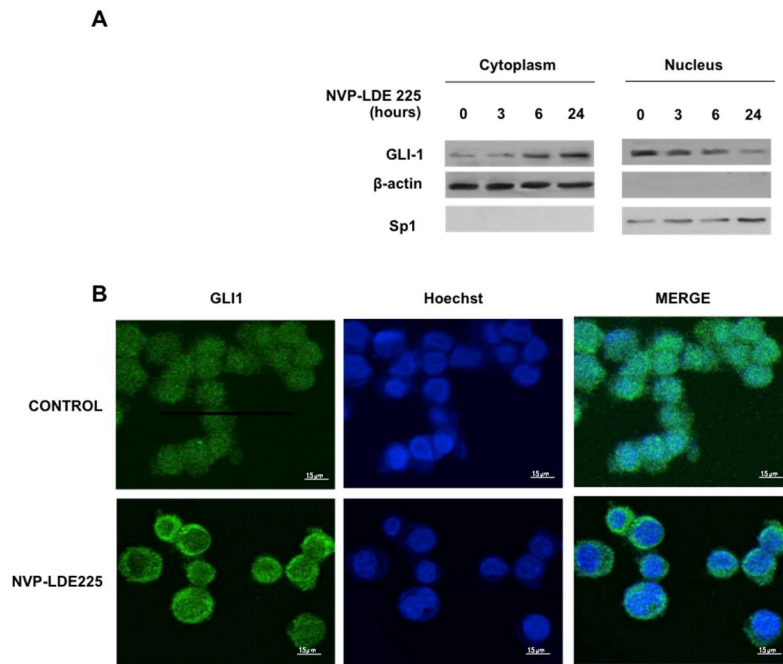


Figure 8. NVP-LDE225 treatment reduces nuclear translocation of GLI1 and increases its cytoplasmic retention.

(A) Western blot analysis of GLI1 on nuclear and cytoplasmic protein extracts from MDA-MB-468 treated with NVP-LDE225 (2.5 μM). β-actin was used as cytoplasmic marker. (B) Intracellular localization of GLI1 protein (green) in MDA-MB-468 treated with NVP-LDE225 (2.5 μM), as analyzed by immunofluorescence analysis. Nuclei are stained in blue (Hoechst). Merged row images show overlapping of Gli1 and Hoechst signals. Scale bars, 15 μm.

NVP-LDE225 increases the efficacy of paclitaxel in nude mice xenografted with TNBC tumors.

Pharmacological inhibition of Hh *in vitro* simultaneously reduces the expression of pro-angiogenic receptors and increases the production of anti-angiogenic secreted factors both in endothelial and TNBC cells. To analyze the overall effect of these findings, an *in vivo* experiment was performed in Balb/C nude mice orthotopically xenografted with MDA-MB-468 cells. We compared the effects of NVP-LDE225 with bevacizumab, each of them combined with paclitaxel; the last combination represents the current standard of care for TNBC patients (Herold and Anders, 2013). As reported in figure 9A, untreated mice reached the maximum allowed tumor size, ca. 2 cm³, on day 63; at this time point, NVP-LDE225 plus paclitaxel and bevacizumab plus paclitaxel produced 55% and 29% of growth inhibition, respectively. Notably, the combination of NVP-LDE225 and paclitaxel caused

a long-lasting antitumor activity, with a tumor size of 1.64 cm³ at the end of the experiment, whereas bevacizumab plus paclitaxel treated mice reached the maximum allowed tumor size on day 84. Comparison of tumor sizes, evaluated by the one-way ANOVA test, was statistically significant for the combination NVP-LDE225 and paclitaxel vs. control ($P \leq 0.05$; Fig. 9A). Consistently, as shown in figure 9B, mice treated with NVP-LDE225 and paclitaxel showed a slightly prolonged median survival compared with those treated with bevacizumab and paclitaxel, since 20% of NVP-LDE225-paclitaxel treated mice were still alive at the end of the experiment. Median survival in the NVP-LDE225 plus paclitaxel treated mice was significantly longer than in control mice (79.50 vs. 53.50 days, $P = 0.0089$) (Fig. 9B and Table 5). NVP-LDE225 based treatment was well tolerated; no weight loss or other signs of acute or delayed toxicity were observed. Western blot analysis of tumors from mice sacrificed on day 21, after 2 weeks of treatment, demonstrated that NVP-LDE225 combined with paclitaxel efficiently interfered with Hh-dependent signal transduction by reducing expression of cyclin D1 and Bcl2, both direct targets of GLI1 (Fig. 9C). Interestingly, NVP-LDE225 plus paclitaxel treatment was effective in reducing VEGFR2 and augmenting sVEGFR2 expression, consistently with *in vitro* findings (Fig. 9C). Furthermore, NVP-LDE225 combined with paclitaxel was able to reduce human VEGF-A in mice serum (Fig. 9D). Conversely, an overexpression of THBS1 was found in sera collected from NVP-LDE225 plus paclitaxel treated mice (Fig. 9E). The treatment induced sVEGFR2 secretion by both stromal (mouse sVEGFR2) and tumor cells (human sVEGFR2) (Fig. 9F, 9G).

Immunohistochemical analysis on tumors from mice sacrificed on day 21, after 2 weeks of treatment, demonstrated that NVP-LDE225 combined with paclitaxel interferes with angiogenesis in nude mice xenografted with TNBC tumors. In fact, the combination NVP-LDE225 plus paclitaxel reduced the expression of VEGFR2, NRP2, and CD31, as well as of the proliferation marker Ki67, more efficiently than the combination bevacizumab plus paclitaxel (Fig. 10).

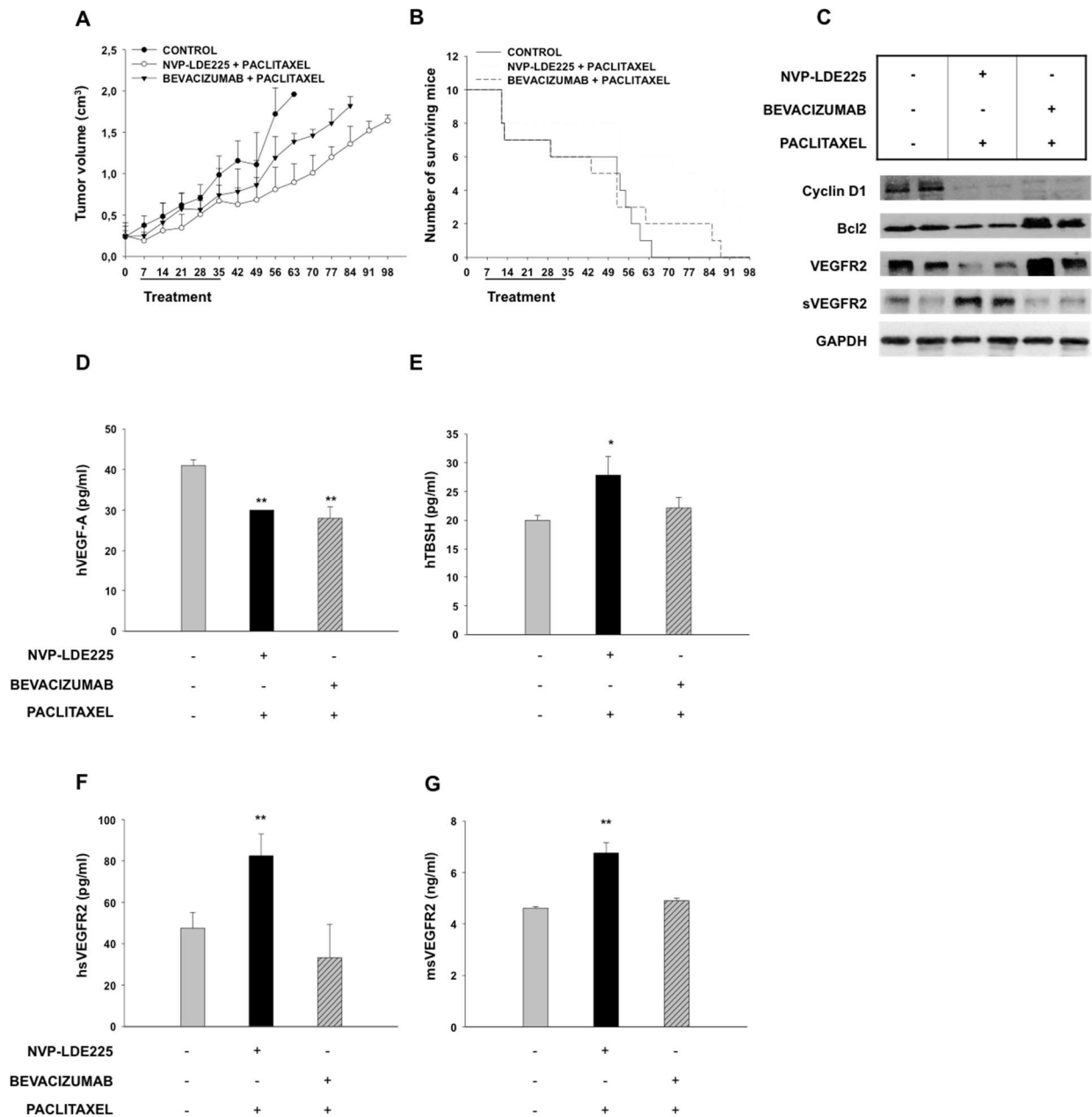


Figure 5. NVP-LDE225 increases efficacy of paclitaxel in nude mice xenografted with TNBC tumors.

(A) Tumor volume of MDA-MB-468 orthotopic xenografts in nude mice, randomized (10/group) to receive NVP-LDE225 or bevacizumab in combination with paclitaxel, as described in the Methods section. The one-way ANOVA test was used to compare tumor sizes among treatment groups at the median survival time of the control group (35 days). Comparison of tumor sizes, evaluated by the one-way ANOVA test, was statistically significant for the combination NVP-LDE225 and paclitaxel vs control ($P \leq 0.05$). (B) Number of surviving mice orthotopically xenografted with MDA-MB-468, after treatments with NVP-LDE225 or bevacizumab in combination with paclitaxel, as described in the Methods section. Median survival differences were statistically significant. Median survival in the NVP-LDE225 plus paclitaxel treated mice was significantly longer than in control mice (79.50 vs 53.50 days, $P = 0.0089$, log-rank test). (C) Western

blot analysis on total lysates from MDA-MB-468 tumor specimens of mice sacrificed on day 21, after two weeks of treatment with NVP-LDE225 or bevacizumab in combination with paclitaxel. **(D, E, F, G)** ELISA assay for determination of **(D)** hVEGF-A, **(E)** hTHSB1, **(F)** hsVEGFR2 and **(G)** msVEGFR2 concentrations (pg/ml) in mice sera, collected on day 21. Data represent the mean (\pm SD) of three independent experiments, each performed in triplicate.

Bars, SDs. Asterisks indicate statistical significance, as determined by the Student t-test ($*P < 0.05$, $**P < 0.01$).

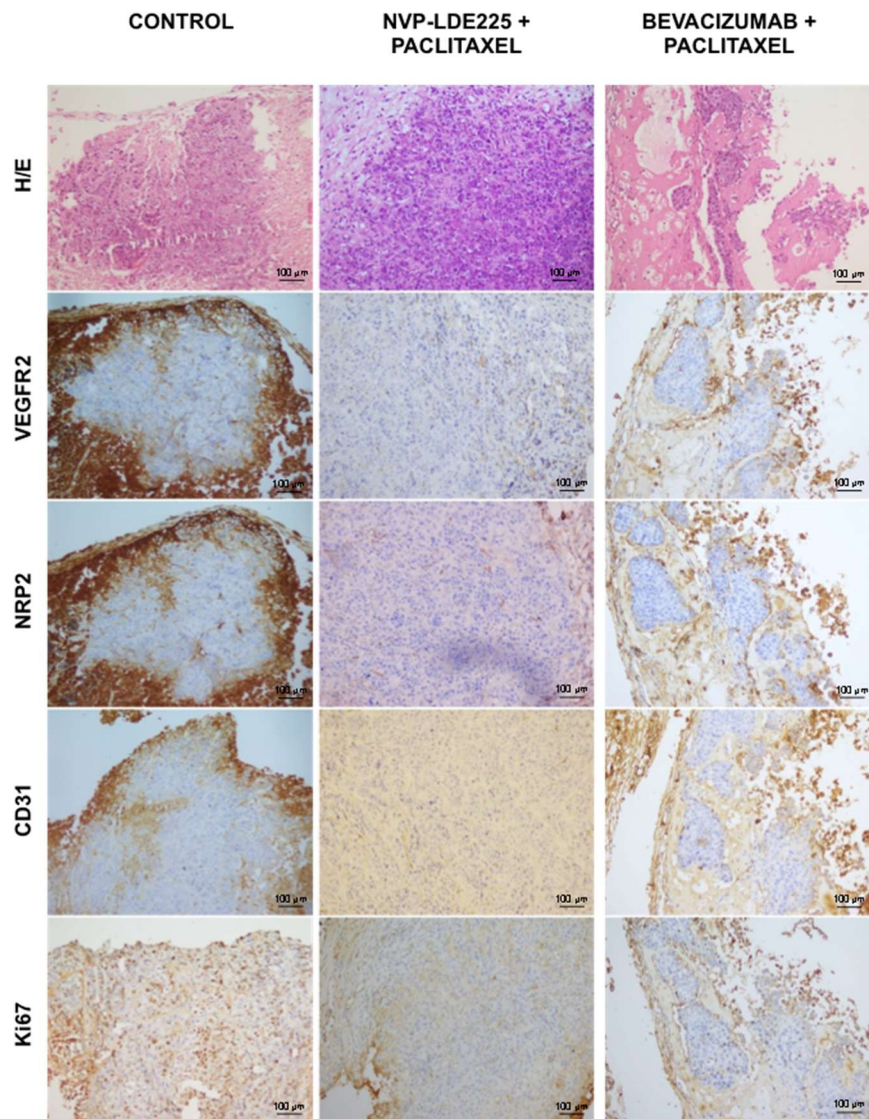


Figure 10. NVP-LDE225 treatment interferes with angiogenesis in nude mice xenografted with TNBC tumors. Immunohistochemical analysis of MDA-MB-468 tumor specimens of mice sacrificed on day 21, after two weeks of treatment with NVP-LDE225 or bevacizumab in combination with paclitaxel, as described in the Methods section. H/E: haematoxylin/eosin staining. Scale bars, 100µm.

Table 5. Comparison of survival curves in nude mice xenografted with TNBC tumors.

Log-rank (Mantel-Cox) Test	
Chi square	6.847
df	1
P value	0.0089
P value summary	**
Are the survival curves sig different?	Yes
Median survival	
NVP-LDE225 + paclitaxel	79.50
Control	53.50
Ratio	1.486
95% CI of ratio	1.091 to 1.881
Hazard Ratio	
Ratio	0.2225
95% CI of ratio	0.07221 to 0.6858

4.3 Task 3:

GLI1 expression correlates with PDL1 in TNBC patients

Recent studies demonstrated TNBCs are more immunogenic compared to the other breast cancer types and express higher levels of PDL1 than nTNBCs (Issam et al., 2018). Since our findings suggested Hh pathway activation in TNBC compared to non TNBC, we explore the potential link between tumor-immune microenvironment of TNBC and Hh signaling.

To evaluate the correlation of Hh pathway activation and PDL1 expression, PDL1 expression was assessed in the TNBC TMA previously evaluated for GLI1 expression. The evaluable cases in which we can analyze both PDL1 and GLI1 protein were 203/237. As shown in 77/203 cases (38.0%) there was a positivity for PDL1 expression; 126/203 cases (62.0%) were negative for PDL1 expression. Notably, among the 77 PDL1-positive samples, 42/77 were also positive for GLI1 (54.5%). Statistical analysis demonstrated a direct significant association between PDL1 and GLI1 expression in TNBC patients ($P = 0.000$, R Pearson = 0.000), as shown in Table 6.

Furthermore we interrogated the open-access database *cBioPortal for Cancer Genomics* in order to explore correlations between other Hh pathway members and PDL1 in TNBCs ; as shown in figure 10 A and 10 B. SMO and PTCH1 mRNA are significantly overexpressed in PDL1 positive TNBCs (Q-value 0.018 and 0.010) .

Table 6. Correlation of GLI1 with PDL1 in TNBC TMA.

		PDL1		Totale
		Neg	Pos	
Gli1	Neg	90	35	125
	Pos	36	42	78
Totale		126	77	203

Chi-quadrato					
	Valore	df	Sig. asint. (2 vie)	Sig. esatta (2 vie)	Sig. esatta (1 via)
Chi-quadrato di Pearson	13,628 ^a	1	,000		
Correzione di continuità ^b	12,552	1	,000		
Rapporto di verosimiglianza	13,565	1	,000		
Test esatto di Fisher				,000	,000
Associazione lineare-lineare	13,561	1	,000		
N. di casi validi	203				

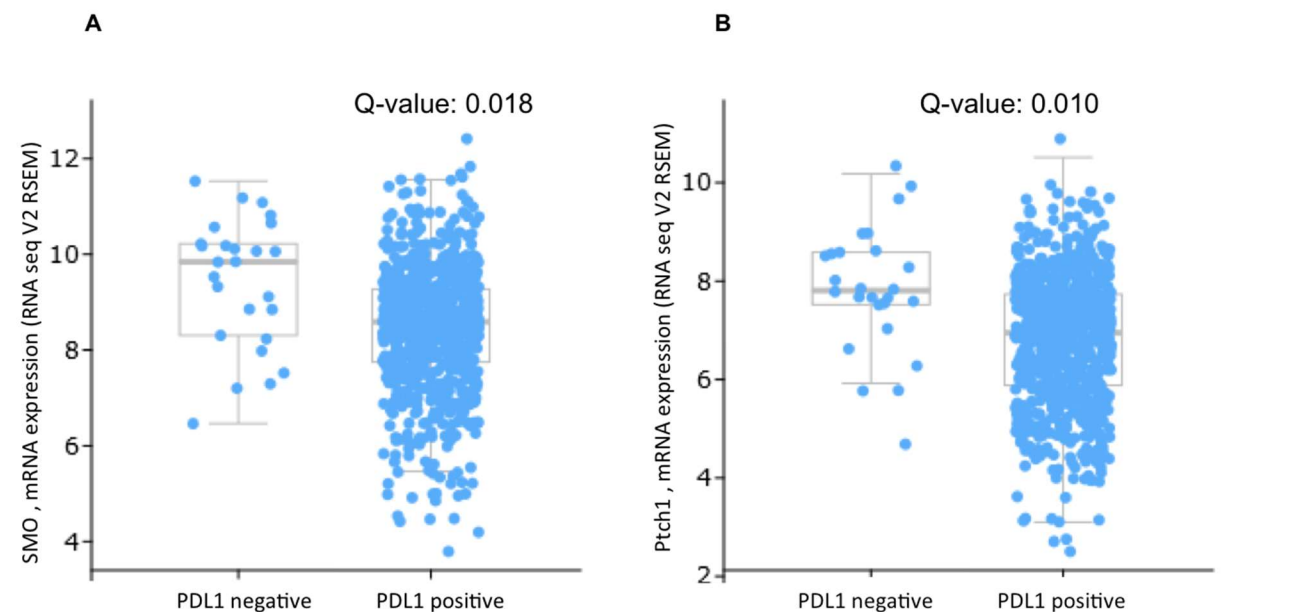


Figure 10. Correlation of SMO and PTCH1 with PDL1. The interactive correlations between SMO, PTCH1 and PDL1 were evaluated interrogating the open-access cBioPortal data sets.

GLI1 regulates PDL1 expression in TNBC cell lines.

To investigate the capability of Hh pathway to modulate components of immune check-point, the expression of PDL1 has been measured: after treatment with NVP-LDE225 a reduction of protein and mRNA levels was observed in all TNBC cell lines evaluated (Fig. 11A, 11B). The NVP-LDE225 pharmacological modulation of PDL1 protein and RNA was evaluated also in MDA-MB-468 tumor specimens of previous *in vivo* experiment (Fig. 11C, 11D). We hypothesized that Hh could be involved in the transcriptional modulation of the PDL1, eventually mediated by GLI1. To address this issue, GLI1 overexpression was performed in MDA-MB-231, a TNBC cell line with a low endogenous expression of GLI1. The levels of PDL1 protein increased slightly when GLI1 was overexpressed, probably due to high basal levels of endogenous PDL1 as shown in figure 11E. Therefore GLI1 overexpression was induced in HCC70 cell lines, a TNBC model with lower endogenous level of both GLI1 and PDL1 than other TNBC cells. As shown in figure 11F, PDL1 protein clearly augmented when GLI1 was overexpressed. A bioinformatic analysis looking for the promoter regions for PDL1 revealed two regulatory regions upstream of VEGFR2 transcription start site (Fig. 11G). To evaluate the functional GLI1/PDL1 promoter interaction we carried out a chromatin immunoprecipitation analysis for GLI1 followed by PCR amplification of two different regions (P1 and P2) of the PDL1 gene promoter. We found that GLI1 binds the PDL1 promoter, especially in the P1 region. To confirm that GLI1 transcriptionally enhances PDL1 a luciferase reporter assay will be performed (fig. 11H).

The expression of GLI1 was evaluated in 4T1 cells, a TNBC murine model that when injected into BALB/c mice spontaneously produces highly metastatic tumors. As shown in figure 12A, 4T1 cells viability was inhibited by NVP LDE 225 treatment in a dose-dependent manner; also the treatment with GANT61, a direct GLI1 antagonist, decreased 4T1 cells proliferation (Fig. 12B). NVP-LDE225

treatment was effective in reducing PDL1 protein expression as well as cyclin D1, well-known target of GLI1 (Fig.12C). To analyze the overall effect of these *in vitro* findings, an *in vivo* experiment will be performed in Balb/C mice orthotopically xenografted with 4T1 cells.

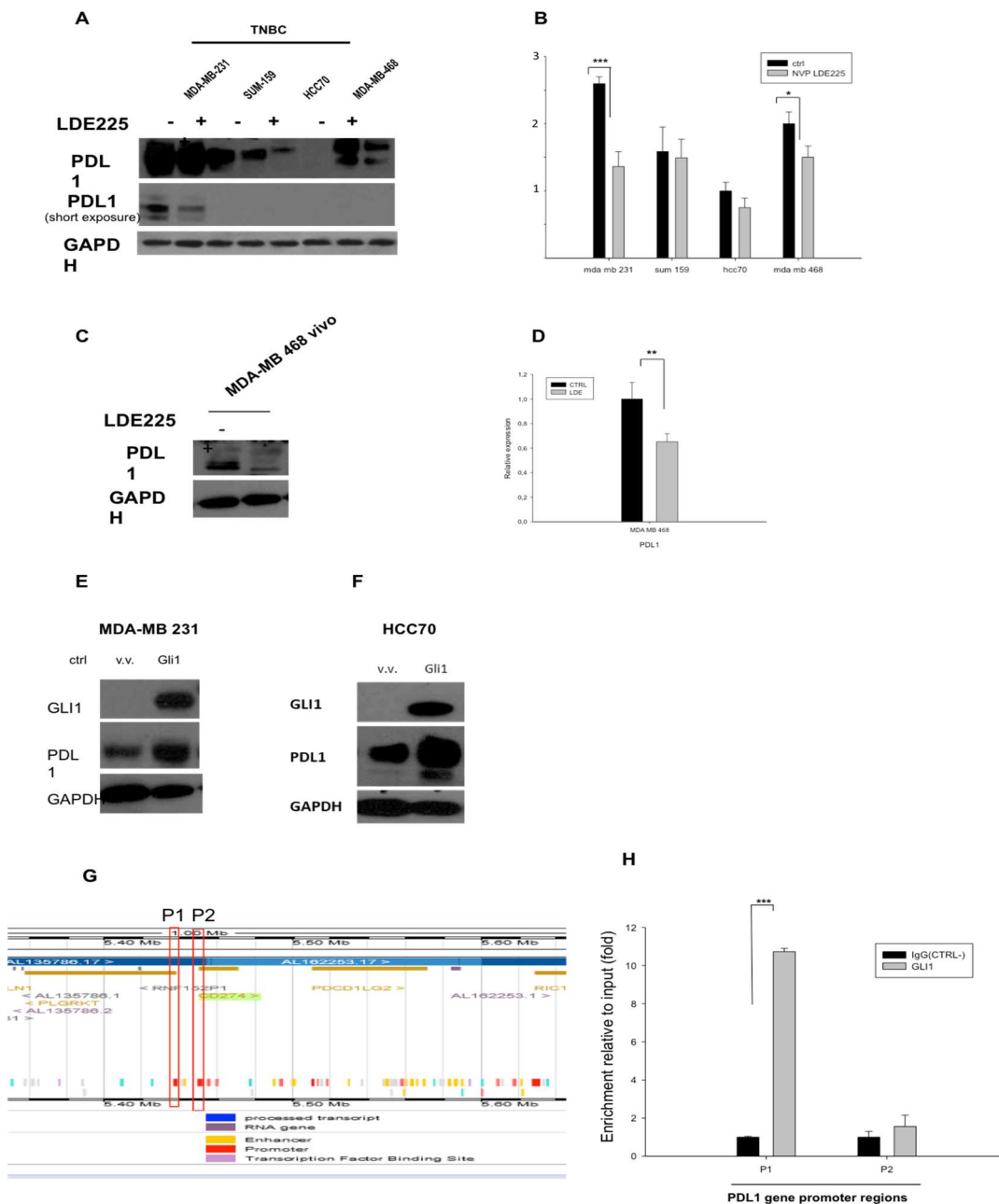


Figure 11. Hh pathway modulates PDL1 expression in TNBC cell lines. (A) Western blot analysis of protein expression in TNBC cells treated with NVP-LDE225 (2.5 μ M). (B) Relative expression of PDL1 mRNA in TNBC cells treated with NVP-LDE225 (2.5 μ M), as performed by Real Time RT-PCR (qRT-PCR) analysis. Data were calculated with mean cycle threshold (CT) values, normalised to endogenous control. Data represent the mean (\pm SD) of three

independent experiments, each performed in triplicate. (C-D) Western blot analysis of protein expression in MDA-MB-468 tumor specimen after 21 days of NVP-LDE225 treatment in in vivo experiment (D) Relative expression of PDL1 mRNA in MDA-MB-468 tumor specimen after 21 days of NVP-LDE225 treatment in in vivo experiment . (E-F) Western blot analysis of protein expression in MDA-MB-231 cells (E) and in HCC70 (F), 24 hours after transfection with either pCMV6-GFP empty vector, pCMV6-GFP GLI1 plasmids using lipofectamine 2000 in DMEM. (G) two regulatory promoter region of PDL1 gene are highlighted in red and named P1 and P2. (H) Chromatin immunoprecipitation (ChIP) assay in MDA-MB-468 cells by using a GLI1 antibody and primers specific for the PDL1 promoter. Results were reported as fold change compared to negative control (IgG antibody); results were the average of three independent experiments. Bars, SDs. Asterisks indicate statistical significance, as determined by the Student t-test.

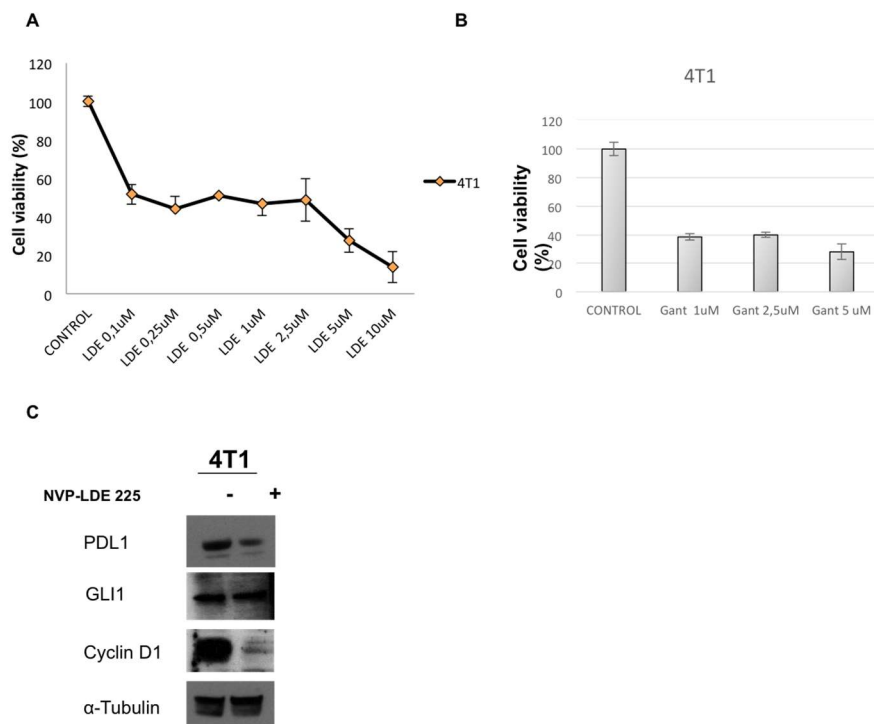


Figure 12. Hh pathway inhibition exerts antiproliferative effects on 4T1 breast cancer cells. (A) Effects of NVP-LDE225 and **(B)** GANT61 treatment on 4T1 cells viability measured by MTT assay, **(C)** Western blot analysis of protein expression in 4T1 cells treated with NVP-LDE225 (2.5 μ M).

5. Discussion

Breast cancers which lack the expression of ER, PgR, and HER2 receptors are grouped and defined as TNBCs. Owing to the lack of targeted therapies, these cancers are uniformly treated with chemotherapy (Cleator and Heller, 2007); nevertheless, outcomes are poor compared with those of other subtypes (Mustacchi and De Laurentis, 2015).

Despite considered a single entity from a clinical perspective, TNBC is a heterogeneous disease which comprises distinct molecular subtypes (Bose, 2015). The difficulties encountered to identify several targetable molecules in TNBC are based on common and wrong idea of TNBC as a single entity. In the last decade research efforts have focused on sub-divided TNBC in smaller groups, bearing similar molecular features and sharing uniform oncogenic behaviour (Pareja F et al, 2016; Shah et al., 2012). Higher expression of different biomarkers including VEGFR, epidermal growth factor receptor (EGFR) and fibroblast growth factor receptor (FGFR), has given the rationale for clinical trials assessing the role of targeted inhibitors to these pathways in triple-negative tumors (Andreopoulou et al., 2012). Results from these trials have shown some benefit in small subgroups of patients, which reflects the heterogeneity of TNBC (Arnedos et al., 2012) and highlights the need for a further sub-classification of these tumors for better prognosis assessment and treatment individualization.

Furthermore there are growing evidences that TNBCs, characterized by a high level of immune cells infiltration, are more immunogenic compared to other breast cancers, encouraging researchers to investigate TNBC response to immune check-point inhibitors. The complex interactions between TILs and tumor cells in TNBC represent an area of interest and remain not well characterized.

Several studies suggest the involvement of Hh pathway in breast cancer (O'Toole et al., 2011), although the functional significance of these findings and their potential therapeutic impact is unclear. In our work, we found that TNBC cells overexpress the Hh family transcription factors GLI1 and

tGLI1. In a tissue microarray analysis on 200 TNBC patients, about 12% and 26% of patients expressed the GLI1 protein at low and moderate levels, respectively.

Since it is known that the Hh pathway promotes cancer progression influencing the surrounding microenvironment through epithelial-stromal interaction (Yauch et al., 2008; Theunissen and de Sauvage, 2009; Heller et al., 2012), we deeply explored the effect of GLI1/tGLI1 overexpression in TNBC initiated angiogenesis and we began to characterize the function of Hh pathway in TNBC immune escape mechanisms.

Interestingly, a statistically significant association between VEGFR2 and GLI1 expression was found in TNBC patients. In *in vitro* experiments we highlighted that overexpressing GLI1 cancer cells influenced endothelial cells proliferation and their capability to form capillary, in part regulating the VEGF-A production as previously described. Despite Hh inhibition depressed VEGF-A secretion less efficiently than the anti-VEGF monoclonal antibody bevacizumab, we found that NVP-LDE225 discouraged capillary organization in a more evident manner. With the intent to demonstrate that the Hh pathway could regulate tumor angiogenesis in both VEGF-dependent and VEGF-independent manners, we found an upregulation of sVEGFR2 and THBS1 after pharmacological Hh pathway inhibition. sVEGFR2 represents a VEGFR2 splicing variant identified as an endogenous inhibitor of lymphangiogenesis; it acts as a decoy receptor, sequestering VEGF from VEGFR-2 binding (Albuquerque et al., 2009; Shibata et al., 2010). THBS1 represents a natural anti-angiogenic secreted factor (Lawler, 2002; Henkin and Volpert, 2011). Collectively, the reduction of VEGF-A, coupled with the upregulation of sVEGFR2 and THBS1, could explain the deeper antiangiogenic *in vitro* effect of NVP-LDE225 compared to bevacizumab, since the latter is able to only suppress VEGF-A activated angiogenesis. Simultaneously with the increase of sVEGFR2, reduced levels of VEGFR2 protein and mRNA were found after Hh inhibition, thus suggesting a putative regulation of VEGFR2 expression by Hh. As hypothesized by bioinformatic analysis, we demonstrated a functional interaction between tGLI1 and the VEGFR2 promoter, demonstrating a transcriptional modulation of the VEGFR2 receptor mediated by tGLI1.

These findings suggest that GLI1/tGLI1 overexpressing cancer cells promote tumor progression in a paracrine manner. They can orchestrate tumor vascularization not only by inducing VEGF-A secretion but also by upregulating VEGFR2 on cancer cell surface, thus establishing a secreted factors/receptors autocrine loop. The Hh pathway could regulate other angiogenic receptors: for instance, Lal Goel and colleagues demonstrated that GLI1 sustains a NRP2/ α 6 β 1 integrin based autocrine loop through enhanced NRP2 expression (Goel et al., 2013). Increased production of THBS1 and sVEGFR2 strengthens the anti-angiogenic effects observed upon Hh inhibition. Collectively, our data suggest that HH pathway activation in TNBC cellular models acts on tumour angiogenesis in a wide manner and at multiple levels. Promoting production and interactions between several pro-angiogenic secreted or receptor factor, HH signalling is able to equip the TNBCs of vascular structures that facilitate tumor progression and metastasis. Therefore, it is possible that Hh pharmacological inhibition discourages the pro-angiogenic behavior of TNBC.

These data are in part confirmed by the finding that, in tumor samples of TNBC patients, VEGFR2 expression correlated with GLI1 expression. This co-expression reflects the functional connection between the transcriptional factor and the receptor identified in *in vitro* analysis. Therefore, co-expressing GLI1 and VEGFR2 TNBC might be considered a new subgroup in which Hh pathway inhibition could be clinically investigated because of its effects on both cancer cells and tumor microenvironment.

To evaluate the translational relevance of these findings, the combinations of paclitaxel with either NVP-LDE225 or bevacizumab were tested in TNBC xenografted mice. Whereas bevacizumab administration remains controversial, especially because of small clinical benefits and high costs associated, its combination with paclitaxel represents the canonical schedule for TNBC treatment. By scheduling NVP-LDE225 rather than bevacizumab, we attempted to demonstrate the therapeutic advantage of this combination. In line with the findings that NVP-LDE225 seems to act as a multi anti-angiogenic drug, modulating both secreted factors and receptors involved in angiogenesis, mouse serum levels of circulating VEGF-A were decremented upon NVP-LDE225 administration. In

addition, the treatment induced an overproduction of THBS1 from tumor cells and of sVEGFR2 from both tumor (h-sVEGFR2) and endothelial (m-sVEGFR2) cells, events associated with discouraged neovascularization and metastatic potential inhibition (Albuquerque et al., 2009; Henkin and Volpert, 2011). VEGFR2 levels on tumor surface were deeply reduced as well as some proliferation markers such as pERK. Collectively, the combination of NVP-LDE225 and paclitaxel provides a better sustained inhibition of both tumor cells proliferation and endothelial cells organization.

Since PDL1 is frequently overexpressed in TNBC patients and our findings demonstrated an activation of Hh pathway in this subset of tumors, we speculate about the potential link between tumor-immune microenvironment of TNBC and Hh signaling.

Surprisingly a statistically significant association between PDL1 and GLI1 expression was found in TNBC patients TMA. We also evaluated the potential correlation between SMO and PTCH1 receptors, other members of Hh signaling, and PDL1 interrogating the cBIOportal database. A significant overexpression of both receptors was found in PDL1 positive TNBC patients.

In *in vitro* experiments we found that PDL1 protein and mRNA levels decreased after pharmacological Hh pathway inhibition. Based on these data we hypothesized that Hh activation enhanced immune-escape via up-regulation PDL1. In our cellular models we demonstrated a physical interaction between GLI1 and the PDL1 promoter; luciferase reporter assay will confirm the functional modulation of the PDL1 mediated by GLI1.

In order to evaluate the effects of Hh inhibition on anti-tumor immune-response we plan to perform an *in vivo* experiment in Balb-C immune-competent mice xenografted with a murine TNBC cell line. For this purpose, Hh pathway activation and Hh inhibitors sensitivity were tested in 4T1 TNBC murine cells. *In vitro* analyses demonstrated that 4T1 cells express GLI1 and that are responsive to Hh pathway inhibitors. In 4T1 xenografted Balb-C mice we will evaluate the effects of Hh pathway activation on immune features of the tumor microenvironment and the effect of Hh inhibition and immunotherapy combined strategy.

Our data support the clinical development of novel pharmacological combinations that include Hh blockade, especially those that could potentiate anti-angiogenic or immunomodulatory effects. Due to their ability to target both tumor cells and the pro-tumor microenvironment, Hh inhibitors represent promising therapeutics to be clinically investigated in GLI1 overexpressing TNBC patients.

6. References

- Albuquerque RJ, Hayashi T, Cho WG, Kleinman ME, Dridi S, Takeda A, Baffi JZ, Yamada K, Kaneko H, Green MG, Chappell J, Wilting J, Weich HA, Yamagami S, Amano S, Mizuki N, Alexander JS, Peterson ML, Brekken RA, Hirashima M, Capoor S, Usui T, Ambati BK, Ambati J. (2009). Alternatively spliced vascular endothelial growth factor receptor-2 is an

- essential endogenous inhibitor of lymphatic vessel growth. *Nat Med.*; **15**:1023-30, doi: 10.1038/nm.2018.
- André F, Job B, Dessen P, Tordai A, Michiels S, Liedtke C, Richon C, Yan K, Wang B, Vassal G, Delaloge S, Hortobagyi GN, Symmans WF, Lazar V, Pusztai L (2009). Molecular characterization of breast cancer with high-resolution oligonucleotide comparative genomic hybridization array. *Clin Cancer Res* **15**: 441-51, doi: 10.1158/1078-0432.CCR-08-1791.
 - Andreopoulou E, Schweber SJ, Sparano JA, McDavid HM (2015) Therapies for triple negative breast cancer. *Expert Opin Pharmacother*; **16**:983-98.
 - Angelucci C, Maulucci G, Lama G, Proietti G, Colabianchi A, Papi M, Maiorana A, De Spirito M, Micera A, Balzamino OB, Di Leone A, Masetti R, Sica G. (2012). Epithelial-stromal interactions in human breast cancer: effects on adhesion, plasma membrane fluidity and migration speed and directness. *PLoS One*; **7**: e50804, doi: 10.1371/journal.pone.0050804.
 - Ann Hanna, Brandon J. Metge, Sarah K. Bailey, Dongquan Chen, Darshan S. Chandrashekar, Sooryanarayana Varambally, Rajeev S. Samant & Lalita A. Shevde. Inhibition of Hedgehog signaling reprograms the dysfunctional immune microenvironment in breast cancer- Dec 2018- Oncoimmunology.
 - Arnedos M, Bihan C, Delaloge S, and Andre F (2012). Triple-negative breast cancer: are we making headway at least? *Ther Adv Med Oncol*; **4**:195-210, doi: 10.1177/1758834012444711.
 - Atsushi Otsuka¹, Jil Dreier¹, Phil F. Cheng¹, Mirjam Naegeli¹, Holger Lehmann², Lea Felderer¹, Ian J. Frew², Shigeto Matsushita^{1,3}, Mitchell P. Levesque¹, and Reinhard Dummer¹ Hedgehog Pathway Inhibitors Promote Adaptive Immune Responses in Basal Cell Carcinoma. *Clinical cancer research* January 15, 2015; DOI: 10.1158/1078-0432.CCR-14-2110 .
 - Bear HD, Tang G, Rastogi P, Geyer CE Jr, Robidoux A, Atkins JN, Baez-Diaz L, Brufsky AM, Mehta RS, Fehrenbacher L, Young JA, Senecal FM, Gaur R, Margolese RG, Adams PT,

- Gross HM, Costantino JP, Swain SM, Mamounas EP, Wolmark N (2012). Bevacizumab added to neoadjuvant chemotherapy for breast cancer. *N Engl J Med* **366**:310-20, doi: 10.1056/NEJMoa1111097.
- Bose S (2015). Triple-negative Breast Carcinoma: Morphologic and Molecular Subtypes. *Adv Anat Pathol*; **22**:306-13, doi: 10.1097/PAP.0000000000000084.
 - Cao X, Geradts J, Dewhirst MW, Lo HW (2012). Upregulation of VEGF-A and CD24 Gene Expression by the tGLI1 Transcription Factor Contributes to the Aggressive Behavior of Breast Cancer Cells. *Oncogene*; **31**:104-15, doi: 10.1038/onc.2011.219.
 - Carpenter RL, Lo HW (2012). Hedgehog Pathway and GLI1 Isoforms in Human Cancer. *Discov Med*; **13**:105–13.
 - Chacón RD and Costanzo MV (2010). Triple-negative breast cancer. *Breast Cancer Res*; **12** Suppl 2:S3, doi: 10.1186/bcr2574.
 - Cleator S, Heller W, Coombes RC (2007). Triple-negative breast cancer: therapeutic options. *Lancet Oncol*; **8**:235–44.
 - Cohen MM Jr (2010). Hedgehog signaling update. *J Med Genet A*; **152A**:1875-914, doi: 10.1002/ajmg.a.32909.
 - D'Amato C , Rosa R, Marciano R, D'Amato V, Formisano L, Nappi L, Raimondo L, Di Mauro C, Servetto A, Fulciniti F, Cipolletta A, Bianco C, Ciardiello F, Veneziani BM, De Placido S, Bianco R. (2014). Inhibition of Hedgehog signalling by NVP-LDE225 (Erismodegib) interferes with growth and invasion of human renal cell carcinoma cells. *Br J Cancer*; **111**:1168–79, doi: 10.1038/bjc.2014.421.
 - Dent R, Trudeau M, Pritchard KI, Hanna W M, Kahn HK, Sawka CA, Lickley LA, Rawlinson E, Sun P, Narod SA (2007). Triple-Negative Breast Cancer: Clinical Features and Patterns of Recurrence. *Clin Cancer Res*; **13**:4429-34.

- Ferrara N, Hillan KJ, Gerber HP, Novotny W (2004). Discovery and development of bevacizumab, an anti-VEGF antibody for treating cancer. *Nature Reviews Drug Discovery*; **3**:391-400, doi: 10.1038/nrd1381
- Goel HL, Pursell B, Chang C, Shaw LM, Mao J, Simin K, Kumar P, Vander Kooi CW, Shultz LD, Greiner DL, Norum JH, Toftgard R, Kuperwasser C, Mercurio AM (2013). GLI1 regulates a novel neuropilin-2/a6b1 integrin based autocrine pathway that contributes to breast cancer initiation. *EMBO Mol Med.*; **5**:488–508, doi: 10.1002/emmm.201202078.
- Gray R, Bhattacharya S, Bowden C, Miller K, Comis RL (2009). Independent review of E2100: a phase III trial of bevacizumab plus paclitaxel versus paclitaxel in women with metastatic breast cancer. *J Clin Oncol*; **27**(30):4966-72.
- Habib JG, O'Shaughnessy JA (2016). The hedgehog pathway in triple-negative breast cancer. *Cancer Med*; **5**:2989-3006, doi: 10.1002/cam4.833.
- Haffty BG, Yang Q, Reiss M, Kearney T, Higgins SA, Weidhaas J, Harris L, Hait W, Toppmeyer D (2006). Locoregional relapse and distant metastasis in conservatively managed triple negative early-stage breast cancer. *J Clin Oncol*; **24**:5652–57.
- Harris LG, Pannell LK, Singh S, Samant RS, Shevde LA (2012). Increased vascularity and spontaneous metastasis of breast cancer by hedgehog signaling mediated upregulation of *cyr61*. *Oncogene*; **31**:3370-80, doi: 10.1038/onc.2011.496.
- Heller E, Hurchla MA, Xiang J, Su X, Chen S, Schneider J, Joeng KS, Vidal M, Goldberg L, Deng H, Hornick MC, Prior JL, Piwnica-Worms D, Long F, Cagan R, Weilbaecher KN (2012). Hedgehog signaling inhibition blocks growth of resistant tumors through effects on tumor microenvironment. *Cancer Res.*; **72**:897-907, doi: 10.1158/0008-5472.CAN-11-2681.doi: 10.1158/0008-5472.CAN-11-2681.
- Henkin J, Volpert OV (2011). Therapies using anti-angiogenic peptide mimetics of thrombospondin-1. *Expert Opin Ther Targets*; **15**:1369-86,doi: 10.1517/14728222.2011.640319.

- Herold CI, Anders CK (2013). New targets for triple-negative breast cancer. *Oncology (Williston Park)*; **27**:846-54.
- Hochman E, Castiel A, Jacob-Hirsch J, Amariglio N, Izraeli S. Molecular pathways regulating pro- migratory effects of Hedgehog signaling. *J Biol Chem*. 2006; 281:33860–70. [PubMed: 16943197]
- Ingham, P.W. & McMahon, A.P. Hedgehog signaling in animal development: paradigms and principles. *Genes Dev*. 15, 3059–3087 (2001)
- Issam Makhoul, Mohammad Atiq,Ahmed Alwbari, and Thomas Kieber-Emmons. Breast Cancer Immunotherapy: An Update. *Breast Cancer* 2018; 12: 1178223418774802. doi: 10.1177/1178223418774802v
- Katoh Y, Katoh M (2009). Hedgehog target genes: mechanisms of carcinogenesis induced by aberrant hedgehog signaling activation. *Curr Mol Med*; **9**:873-86.
- Kinzler K W and Vogelstein B (1990). The GLI gene encodes a nuclear protein which binds specific sequences in the human genome. *Mol Cell Biol*; **10**:634–42.
- Lawler J (2002) Thrombospondin-1 as an endogenous inhibitor of angiogenesis and tumor growth. *J Cell Mol Med*.; **6**:1-12.
- Liedtke C, Mazouni C, Hess KR, André F, Tordai A, Mejia JA, Symmans WF, Gonzalez-Angulo AM, Hennessy B, Green M, Cristofanilli M, Hortobagyi GN, Pusztai L (2008). Response to neoadjuvant therapy and long-term survival in patients with triple-negative breast cancer. *J Clin Oncol*; **26**:1275-81, doi: 10.1200/JCO.2007.
- Linderholm BK, Hellborg H, Johansson U, Elmberger G, Skoog L, Lehtiö J, Lewensohn R (2009). Significantly higher levels of vascular endothelial growth factor (VEGF) and shorter survival times for patients with primary operable triple-negative breast cancer. *Ann Oncol*; **20**:1639-46, doi: 10.1093/annonc/mdp062.
- Liu JF, Tolaney SM, Birrer M, et al. A phase 1 trial of the poly (ADP-ribose) polymerase inhibitor olaparib (AZD2281) in combination with the anti-angiogenic cediranib (AZD2171)

- in recurrent epithelial ovarian or triple-negative breast cancer. *Eur J Cancer*. 2013;49(14):2972-8. doi: 10.1016/j.ejca.2013.05.020.
- Miles DW, Chan A, Dirix LY, Cortés J, Pivot X, Tomczak P, Delozier T, Sohn JH, Provencher L, Puglisi F, Harbeck N, Steger GG, Schneeweiss A, Wardley AM, Chlistalla A, Romieu G. (2010). Phase III study of bevacizumab plus docetaxel compared with placebo plus docetaxel for the first-line treatment of human epidermal growth factor receptor 2-negative metastatic breast cancer. *J Clin Oncol*; **20**:3239-47.
 - Mohammed RA, Ellis IO, Mahmmod AM, Hawkes EC, Green AR, Rakha EA, Martin SG (2011) Lymphatic and blood vessels in basal and triple-negative breast cancers: characteristics and prognostic significance. *Mod Pathol*; **24**:774–85.
 - Mustacchi G, De Laurentiis M (2015) Drug Design, Development and Therapy The role of taxanes in triple-negative breast cancer: literature review. *Drug Des Devel Ther*; **9**:4303–18.
 - Nagase T, Nagase M, Machida M, Fujita T (2008). Hedgehog signalling in vascular development. *Angiogenesis*; **11**:71-7, doi: 10.1007/s10456-008-9105-5.
 - Nyberg P, Xie L, Kalluri R (2005). Endogenous Inhibitors of Angiogenesis. *Cancer Res.*; **65**:3967-79.
 - O'Toole SA, Machalek DA, Shearer RF, Millar EK, Nair R, Schofield P, McLeod D, Cooper CL, McNeil CM, McFarland A, Nguyen A, Ormandy CJ, Qiu MR, Rabinovich B, Martelotto LG, Vu D, Hannigan GE, Musgrove EA, Christ D, Sutherland RL, Watkins DN, Swarbrick A (2011). Hedgehog Overexpression Is Associated with Stromal Interactions and Predicts for Poor Outcome in Breast Cancer. *Cancer Res.*; **71**:4002-14, doi: 10.1158/0008-5472.CAN-10-3738.
 - Pak E, Segal RA (2016). Hedgehog Signal Transduction: Key Players, Oncogenic Drivers, and Cancer Therapy. *Dev Cell*; **38**:333-44, doi: 10.1016/j.devcel.2016.07.026.

- Palma G, Frasci G, Chirico A, Esposito E, Siani C, Saturnino C, Arra C, Ciliberto G, Giordano A, D'Aiuto M (2015). Triple negative breast cancer: looking for the missing link between biology and treatments. *Oncotarget*; **6**:26560-74, doi: 10.18632/oncotarget.5306.
- Penault-Llorca F, Viale G (2012). Pathological and molecular diagnosis of triple-negative breast cancer: a clinical perspective. *Ann Oncol*; **23**:vi19–vi22.
- Riku M, Inaguma S, Ito H, Tsunoda T, Ikeda H, Kasai K (2015). Down-regulation of the zinc-finger homeobox protein TSHZ2 releases GLI1 from the nuclear repressor complex to restore its transcriptional activity during mammary tumorigenesis. *Oncotarget*; **7**:5690-701, doi: 10.18632/oncotarget.6788.
- Robert NJ, Diéras V, Glaspy J, Brufsky AM, Bondarenko I, Lipatov ON, Perez EA, Yardley DA, Chan SY, Zhou X, Phan SC, O'Shaughnessy J (2011). RIBBON-1: randomized, double-blind, placebo-controlled, phase III trial of chemotherapy with or without bevacizumab for first-line treatment of human epidermal growth factor receptor 2-negative, locally recurrent or metastatic breast cancer. *J Clin Oncol* ; **10**: 1252-60.
- Rohatgi R, Milenkovic L, Corcoran RB, Scott MP (2009). Hedgehog signal transduction by Smoothed: pharmacologic evidence for a 2-step activation process. *Proc Natl Acad Sci U S A.*; **106**:3196-201, doi: 10.1073/pnas.0813373106.
- Rudin CM (2012). Vismodegib. *Clin Cancer Res*; **18**:3218–22, doi: 10.1158/1078-0432.CCR-12-0568.
- Sekulic A, Migden MR, Oro AE, Dirix L, Lewis KD, Hainsworth JD, Solomon JA, Yoo S, Arron ST, Friedlander PA, Marmur E, Rudin CM, Chang AL, Low JA, Mackey HM, Yauch RL, Graham RA, Reddy JC, Hauschild A (2012). Efficacy and safety of vismodegib in advanced basal-cell carcinoma. *N Engl J Med.*; **366**:2171-9, doi: 10.1056/NEJMoa1113713.
- Shah SP, Roth A, Goya R, Oloumi A, Ha G, Zhao Y, Turashvili G, Ding J, Tse K, Haffari G, Bashashati A, Prentice LM, Khattra J, Burleigh A, Yap D, Bernard V, McPherson A, Shumansky K, Crisan A, Giuliany R, Rosner J, Lai D, Birol I, Varhol R, Tam A, Dhalla N,

- Zeng T, Ma K, Chan SK, Griffith M, Moradian A, Cheng SW, Morin GB, Watson P, Gelmon K, Chia S, Chin SF, Curtis C, Rueda OM, Pharoah PD, Damaraju S, Mackey J, Hoon K, Harkins T, Tadigotla V, Sigaroudinia M, Gascard P, Tlsty T, Costello JF, Meyer IM, Eaves CJ, Wasserman WW, Jones S, Huntsman D, Hirst M, Caldas C, Marra MA, Aparicio S (2012). The clonal and mutational evolution spectrum of primary triple-negative breast cancers. *Nature*; **486**:395-9, doi: 10.1038/nature10933.
- Shahi MH, Afzal M, Sinha S, Eberhart CG, Rey JA, Fan X, Castresana JS (2010). Regulation of sonic hedgehog-GLI1 downstream target genes PTCH1, Cyclin D2, Plakoglobin, PAX6 and NKX2.2 and their epigenetic status in medulloblastoma and astrocytoma. *BMC Cancer*; **10**:614, doi: 10.1186/1471-2407-10-614.
 - Shibata MA, Ambati J, Shibata E, Albuquerque RJ, Morimoto J, Ito Y, Otsuki Y (2010). The endogenous soluble VEGF receptor-2 isoform suppresses lymph node metastasis in a mouse immunocompetent mammary cancer. *BMC Medicine*; **8**:69, doi: 10.1186/1741-7015-8-69.
 - Stanton SE, Adams S, Disis ML. Variation in the incidence and magnitude of tumor-infiltrating lymphocytes in breast cancer subtypes: a systematic review. *JAMA Oncol.* 2016;2(10):1354-1360. doi: 10.1001/jamaoncol.2016.1061)
 - Tao Y, Mao J, Zhang Q, Li L (2011). Overexpression of Hedgehog signaling molecules and its involvement in triple-negative breast cancer. *Oncology letter*; **2**:995–1001.
 - Theunissen JW, de Sauvage FJ (2009). Paracrine Hedgehog signaling in cancer. *Cancer Res.*; **69**:6007-10, doi: 10.1158/0008-5472.CAN-09-0756.
 - van den Brink, G.R. Hedgehog signaling in development and homeostasis of the gastrointestinal tract. *Physiol. Rev.* 87, 1343–1375 (2007).).
 - Varjosalo, M. & Taipale, J. Hedgehog: functions and mechanisms. *Genes Dev.* 22, 2454–2472 (2008).)
 - von Minckwitz G , Eidtmann H, Rezai M, et al; German Breast Group; Arbeitsgemeinschaft Gynäkologische-Onkologie--Breast Study Groups. Neoadjuvant chemotherapy and

- bevacizumab for HER2-negative breast cancer. *N Engl J Med.* 2012;366(4):299-309. doi: 10.1056/NEJMoa1111065.
- Whiteside TL, Demaria S, Rodriguez-Ruiz ME, Zarour HM and Melero I: Emerging opportunities and challenges in cancer immunotherapy. *Clin Cancer Res.* 22:1845–1855. 2016.)
 - Xie, J. *et al.* Activating Smoothed mutations in sporadic basal-cell carcinoma. *Nature* **391**, 90–92 (1998).
 - Yamazaki M, Nakamura K, Mizukami Y, Ii M, Sasajima J, Sugiyama Y, Nishikawa T, Nakano Y, Yanagawa N, Sato K, Maemoto A, Tanno S, Okumura T, Karasaki H, Kono T, Fujiya M, Ashida T, Chung DC, Kohgo Y (2008). Sonic hedgehog derived from human pancreatic cancer cells augments angiogenic function of endothelial progenitor cells. *Cancer Sci*; **99**:1131-8, doi: 10.1111/j.1349-7006.2008.00795.x.
 - Yauch RL, Gould SE, Scales SJ, Tang T, Tian H, Ahn CP, Marshall D, Fu L, Januario T, Kallop D, Nannini-Pepe M, Kotkow K, Marsters JC, Rubin LL, de Sauvage FJ (2008). A paracrine requirement for hedgehog signalling in cancer. *Nature*; **455**:406-10, doi: 10.1038/nature07275.
 - Yu LY, Tang J, Zhang CM, et al. New immunotherapy strategies in breast cancer. *Int J Environ Res Public Health.* 2017;14(1). pii: E68. doi: 10.3390/ijerph14010068.)